General analysis of the charged Higgs sector of the $Y = 0$ triplet-singlet extension of the MSSM at the LHC

Priyotosh Bandyopadhyay[*]

Dipartimento di Matematica e Fisica "Ennio De Giorgi," Università del Salento and INFN-Lecce,
Via Arnesano, 73100 Lecce, Italy

Indian Institute of Technology Hyderabad, Kandi, Sangareddy 502285, Telangana, India

Antonio Costantini[†]

Dipartimento di Matematica e Fisica "Ennio De Giorgi," Università del Salento and INFN-Lecce,
Via Arnesano, 73100 Lecce, Italy

Claudio Corianò[‡]

Dipartimento di Matematica e Fisica "Ennio De Giorgi," Università del Salento and INFN-Lecce,
Via Arnesano, 73100 Lecce, Italy and STAG Research Centre and Mathematical Sciences,
University of Southampton, Southampton SO17 1BJ, United Kingdom
(Received 15 April 2016; published 26 September 2016)

We investigate the extended Higgs sectors, specially the charged Higgs sector, in a supersymmetric $Y = 0$ $SU(2)$ triplet and a Standard Model (SM) gauge singlet extension of the SM. We show that, in this model, the allowed data for the Higgs boson interaction eigenstates tend to group into separate blocks for a $SU(2)$ triplet, doublet, and singlet. A typical mass spectrum has a doublet-type Standard Model like a Higgs of 125 GeV, a tripletlike light charged Higgs boson, and a very light singletlike pseudoscalar, with the rest relatively decoupled. Later, we investigate the different decay processes allowed in a charged Higgs boson of this model. Specifically, we search for new decay modes of the charged Higgs bosons in order to distinguish between Higgs fields belonging to $SU(2)$ doublet and triplet representations, and also to show the existence of a light pseudoscalar which belong to the singlet representation. The different production modes for the light charged Higgs boson have been discussed, including the limiting case of $|\lambda_T| \simeq 0$. We also propose a few final state modes carrying the distinctive signatures of this model which could be investigated at the LHC and future colliders. The signatures of the singlet and/or the triplet can be explored with an earlier reach of 120 fb^{-1} for some final states at the LHC with 14 TeV of center of mass energy.

I. INTRODUCTION

The recently discovered Higgs boson with a mass of around 125 GeV has confirmed the presence of at least one CP-even scalar responsible for the mechanism of electroweak symmetry breaking (EWSB), in agreement with the Standard Model prediction [1–3]. The existence of an extended Higgs sector and its possible contribution to the EWSB mechanism, however, has not been ruled out. In fact, even with its success, the Standard Model is not a complete theory of fundamental interactions. This point of view is supported by various limitations of the theory, with the unsolved gauge hierarchy problem and the mounting evidence in favor of dark matter—which does not find any justification within the model—being just two among several.

Supersymmetric extensions of the SM, even if disfavored in their minimal formulations—such as in constrained minimal supersymmetric extension of SM (MSSM) scenarios—address the two issues mentioned above in a natural way. Specifically, the introduction of a conserved R-parity guarantees that the lightest supersymmetric particle (LSP) takes the role of a dark matter (DM) component [4].

In the MSSM we have two Higgs doublets giving masses to up- and down-type quarks, respectively. After EWSB, we have two CP-even light neutral Higgs bosons, among which one can be the discovered Higgs around 125 GeV, a CP-odd neutral Higgs boson and a charged Higgs boson pair. Observation of a charged Higgs boson will be obvious proof of the existence of another Higgs doublet, which is necessary in the context of supersymmetry.

Searches for the extended Higgs sector by looking for a charged Higgs boson at the LHC are not new. In fact, both the CMS and ATLAS collaborations have investigated scenarios with charged Higgs bosons, even under the assumption of these being lighter than the top quark ($m_{H^\pm} \leq m_t$). In this case, the channel in question has been the $pp \to t\bar{t}$ production channel, with one of the top decaying into $bH^\pm$. In the opposite case of a charged Higgs heavier than the top ($m_{H^\pm} \geq m_t$), the most studied channels have been the

[*]priyotosh.bandyopadhyay@le.infn.it, bpriyo@iith.ac.in
[†]antonio.costantini@le.infn.it
[‡]claudio.coriano@le.infn.it

$bg \to tH^{\pm}$ and $pp \to tbH^{\pm}$ ones, with the charged Higgs decaying into $\tau\nu_{\tau}$ [5,6]. We recall that both doublet-type charged and neutral Higgs bosons couple to fermions with Yukawa interactions which are proportional to the mixing angle of the up- and down-type $SU(2)$ doublets.

The extension of the MSSM with a SM gauge singlet, i.e., the NMSSM [7], has a scalar which does not couple to fermions or gauge bosons and thus changes the search phenomenology. Similar extensions are possible with only $SU(2)$ triplet superfields with $Y = 0 \pm 2$ hypercharges [8–12]. In the case of $Y = 0$, the neutral part of the triplet scalar does not couple to a Z boson and does not contribute to the Z mass, whereas nonzero hypercharge triplets contribute to both the $W^{\pm}$ and the Z mass.

The supersymmetric extensions of the Higgs sectors with Z_3 symmetry have the common feature of a light pseudo-scalar in the spectrum, known as the R axion in the literature. Such a feature is common to NMSSM with Z_3 symmetry [7] and also to extensions with singlet(s) and triplet(s) with appropriate hypercharges [13–16].

In this article we consider an extension of the MSSM with an $SU(2)$ triplet superfield of $Y = 0$ hypercharge and SM gauge singlet superfield, named the TNMSSM [13,14], with Z_3 symmetry. The main motivation to work with a $Y = 0$ triplet is that it is the simplest triplet extension in the supersymmetric context, where the triplet only contributes to the $W^{\pm}$ mass. For a model with nonzero hypercharges, we need at least two triplets and also get constrained from both the $W^{\pm}$ and Z masses [16]. The light pseudoscalar in this model is mostly singlet and hence does not have any coupling to fermions or gauge bosons. For this reason, such a light pseudoscalar is still allowed by the earlier LEP [17] data and the current LHC data [1–3]. Similarly, the triplet-type Higgs bosons also do not couple to fermions [8–11], which still alllows a light tripletlike charged Higgs in charged Higgs searches [5,6], and such Higgs bosons have to be looked for in different production as well as decay modes.

General features of this model have been presented in [13], while a more detailed investigation of the hidden pseudoscalar was discussed by the authors in [14]. Existence of the light pseudoscalar makes the phenomenology of the Higgs sector very rich for both the neutral and the charged sectors, along with other signatures. In the TNMSSM, we have three physically charged Higgs bosons $h^{\pm}_{1,2,3}$, two of which are triplet type in the gauge basis. The neutral part of the Higgs sector has four CP-even ($h_{1,2,3,4}$) and three CP-odd sectors ($a_{1,2,3}$) states. In the gauge basis, two of the CP-even states are doubletlike, one of which should be the discovered Higgs around 125 GeV, one triplet type and one singlet type. For the CP-odd states, there is one doublet type, one triplet type, and one singlet type. Often, it is the singletlike pseudoscalar which becomes very light, which makes the phenomenology very interesting. The mass spectrum often splits into several regions with distinctively doublet/triplet blocks. The goal of our

analysis is to address the main features of this complete spectrum, characterizing its main signatures in the complex environment of a hadron collider.

Our work is organized as follows. In Sec. II we review the model very briefly. We present a scan over the parameter space of the model in light of recent LHC data and discuss the Higgs boson mass hierarchy in Sec. III. The structure of the charged Higgs bosons are detailed in Sec. IV. The new and modified charged Higgs decay modes consider in Sec. V. In Sec. VI various decay branching fractions are shown for all three charged Higgs bosons with the allowed data points, while several production modes at the LHC are contained in Sec. VII. Finally, we discuss in Sec. VIII the prospect for future searches of triplet and extra doublet Higgs bosons at the LHC and possible ways to distinguish scalar states belonging to such different representations of $SU(2)$. We conclude in Sec. IX.

II. THE MODEL

The superpotential of the TNMSSM, W_{TNMSSM}, contains an $SU(2)$ triplet $\hat{T}$ of zero hypercharge ($Y = 0$), together with a SM gauge singlet $\hat{S}$ added to the superpotential of the MSSM.

The triplet superfield and the two Higgs doublets are then expressed as

$$\hat{T} = \begin{pmatrix} \sqrt{\frac{1}{2}}\hat{T}^0 & \hat{T}_2^+ \\ \hat{T}_1^- & -\sqrt{\frac{1}{2}}\hat{T}^0 \end{pmatrix},$$

$$\hat{H}_u = \begin{pmatrix} \hat{H}_u^+ \\ \hat{H}_u^0 \end{pmatrix}, \qquad \hat{H}_d = \begin{pmatrix} \hat{H}_d^0 \\ \hat{H}_d^- \end{pmatrix}. \qquad (1)$$

In the previous expression, $\hat{T}^0$ is a complex neutral superfield, while $\hat{T}_1^-$ and $\hat{T}_2^+$ are the charged Higgs superfields.

The two terms of the superpotential are combined in the form

$$W_{\mathrm{TNMSSM}} = W_{\mathrm{MSSM}} + W_{TS}, \qquad (2)$$

with

$$W_{\mathrm{MSSM}} = y_t \hat{U} \hat{H}_u \cdot \hat{Q} - y_b \hat{D} \hat{H}_d \cdot \hat{Q} - y_\tau \hat{E} \hat{H}_d \cdot \hat{L} \qquad (3)$$

being the superpotential of the MSSM, while

$$W_{TS} = \lambda_T \hat{H}_d \cdot \hat{T} \hat{H}_u + \lambda_S \hat{S} \hat{H}_d \cdot \hat{H}_u + \frac{\kappa}{3}\hat{S}^3 + \lambda_{TS}\hat{S}\mathrm{Tr}[\hat{T}^2]$$

$$(4)$$

accounts for the extended scalar sector which includes a triplet and a singlet superfield. The MSSM Higgs doublets are the only superfields which couple to the fermion multiplet via Yukawa coupling, as in Eq. (3). After

supersymmetry breaking, the theory is also characterized by a discrete Z_3 symmetry. The soft breaking terms in the scalar potential are given by

$$
\begin{aligned}
V_{\text{soft}} = {} & m^2_{H_u}|H_u|^2 + m^2_{H_d}|H_d|^2 + m^2_S|S|^2 + m^2_T|T|^2 \\
& + m^2_Q|Q|^2 + m^2_U|U|^2 + m^2_D|D|^2 \\
& + (A_S S H_d \cdot H_u + A_\kappa S^3 + A_T H_d \cdot T \cdot H_u \\
& + A_{TS} S \text{Tr}(T^2) + A_U U H_U \cdot Q + A_D D H_D \cdot Q \\
& + \text{H.c.}),
\end{aligned}
\tag{5}
$$

while the D terms take the form

$$
V_D = \frac{1}{2} \sum_k g_k^2 (\phi_i^\dagger t^a_{ij} \phi_j)^2.
\tag{6}
$$

As in our previous study, in this case we also assume that all of the coefficients involved in the Higgs sector are real in order to preserve CP invariance. The breaking of the $SU(2)_L \times U(1)_Y$ electroweak symmetry is then obtained by giving real vacuum expectation values (VEVs) to the neutral components of the Higgs field

$$
\langle H_i^0 \rangle = \frac{v_i}{\sqrt{2}}, \qquad \langle S \rangle = \frac{v_S}{\sqrt{2}},
$$
$$
\langle T^0 \rangle = \frac{v_T}{\sqrt{2}}, \qquad i = u, d
\tag{7}
$$

which give mass to the $W^\pm$ and Z bosons,

$$
m_W^2 = \frac{1}{4} g_L^2 (v^2 + 4v_T^2), \qquad m_Z^2 = \frac{1}{4}(g_L^2 + g_Y^2)v^2,
$$
$$
v^2 = (v_u^2 + v_d^2), \qquad \tan\beta = \frac{v_u}{v_d}.
\tag{8}
$$

The presence of $\hat{S}$ and $\hat{T}$ in the superpotential allows a μ term of the form $\mu_D = \frac{\lambda_S}{\sqrt{2}} v_S + \frac{\lambda_T}{2} v_T$. We also recall that the triplet VEV v_T is strongly constrained by the global fit on the measurement of the ρ parameter [18],

$$
\rho = 1.0004^{+0.0003}_{-0.0004},
\tag{9}
$$

which restricts its value to $v_T \leq 5$ GeV. The nonzero triplet contribution to the $W^\pm$ mass leads to a deviation of the ρ parameter,

$$
\rho = 1 + 4\frac{v_T^2}{v^2}.
\tag{10}
$$

As in [13], in our current numerical analysis we have chosen $v_T = 3$ GeV. The detailed minimization conditions both at tree level and at one loop are given in [13]. We also present the tree-level expressions for the neutral and charged Higgs mass matrices in the Appendix.

III. A SCAN OVER THE PARAMETER SPACE AND THE LHC SELECTION CRITERIA

The main goal of our previous works and of our current one is to search for a suitable region of parameter space, in the form of specific benchmark points, which could allow one or more hidden Higgs particles, compatible with the current LHC limits.

As has already been pointed out [13,14], there are four CP-even neutral (h_1, h_2, h_3, h_4), three CP-odd neutral (a_1, a_2, a_3), and three charged Higgs bosons ($h_1^\pm, h_2^\pm, h_3^\pm$). In general, the interaction eigenstates are obtained via a mixing of the two Higgs doublets, the triplet, and the singlet scalar. However, the singlet does not contribute to the charged Higgs bosons, which are mixed states generated only by the $SU(2)$ doublets and triplets. The rotation from gauge eigenstates to the interaction eigenstates are

$$
\begin{aligned}
h_i &= \mathcal{R}^S_{ij} H_j \\
a_i &= \mathcal{R}^P_{ij} A_j \\
h_i^\pm &= \mathcal{R}^C_{ij} H_j^\pm,
\end{aligned}
\tag{11}
$$

where the eigenstates on the left-hand side are interaction eigenstates, whereas the eigenstates on the right-hand side are gauge eigenstates. Explicitly, we have $h_i = (h_1, h_2, h_3, h_4)$, $H_i = (H_{u,r}^0, H_{d,r}^0, S_r, T_r^0)$, $a_i = (a_0, a_1, a_2, a_3)$, $A_i = (H_{u,i}^0, H_{d,i}^0, S_i, T_i^0)$, $h_i^\pm = (h_0^\pm, h_1^\pm, h_2^\pm, h_3^\pm)$, and $H_i^+ = (H_u^+, T_2^+, H_d^{-*}, T_1^{-*})$. Using these definitions, we can write the doublet and triplet fraction for the scalar and pseudoscalar Higgs bosons as

$$
h_i|_D = (\mathcal{R}^S_{i,1})^2 + (\mathcal{R}^S_{i,2})^2, \qquad a_i|_D = (\mathcal{R}^P_{i,1})^2 + (\mathcal{R}^P_{i,2})^2
\tag{12}
$$

$$
h_i|_S = (\mathcal{R}^S_{i3})^2, \qquad a_i|_S = (\mathcal{R}^P_{i3})^2
\tag{13}
$$

$$
h_i|_T = (\mathcal{R}^S_{i4})^2, \qquad a_i|_T = (\mathcal{R}^P_{i4})^2
\tag{14}
$$

and the triplet and doublet fraction of the charged Higgs bosons as

$$
h_i^\pm|_D = (\mathcal{R}^C_{i1})^2 + (\mathcal{R}^C_{i3})^2, \qquad h_i^\pm|_T = (\mathcal{R}^C_{i2})^2 + (\mathcal{R}^C_{i4})^2.
\tag{15}
$$

We call a scalar (pseudoscalar) Higgs boson doubletlike if $h_i|_D(a_i|_D) \geq 90\%$, singletlike if $h_i|_S(a_i|_S) \geq 90\%$, and tripletlike if $h_i|_T(a_i|_T) \geq 90\%$. Similarly, a charged Higgs boson will be doubletlike if $h_i^\pm|_D \geq 90\%$, or tripletlike if $h_i^\pm|_D \geq 90\%$.

If the discovered Higgs is the lightest CP-even boson, $h_1 \equiv h_{125}$, then h_1 must be doubletlike and the lightest CP-odd and charged Higgses must be triplet- or singletlike in order to evade the experimental constraint from LEP [17]

for the pseudoscalar and charged Higgses. LEP searched for the Higgs boson via the $e^+e^- \rightarrow Zh$ and $e^+e^- \rightarrow h_1h_2$ channels (in models with multiple Higgs bosons) and their fermionic decay modes ($h \rightarrow \bar{b}b$, $\bar{\tau}\tau$ and $Z \rightarrow \ell\ell$). The higher center of mass energy at LEP II (210 GeV) allowed to set a lower bound of 114.5 on the SM-like Higgs boson and of 93 GeV for the MSSM-like Higgs boson in the maximal mixing scenario [17]. Interestingly, neither the triplet- nor the singlet-type Higgs boson couple to Z or to leptons [see Eq. (4)], and we checked explicitly to ensure that the demand of a $\geq 90\%$ singlet and/or triplet is sufficient for the light pseudoscalar to be allowed by LEP data. We also checked explicitly to see that the LHC allowed parameter space for the light pseudoscalar and the details can be found out in [14]. Later, we also discuss how the criteria of a $\geq 90\%$ singlet/triplet is enough to fulfill the constraints coming from the B observables. Similar constraints on the structure of the Higgses must be imposed if $h_2 \equiv h_{125}$. To scan the parameter space, we have used a code written by us in which we have randomly selected 1.35×10^6 points that realize the EWSB mechanism at tree level. Specifically, we have performed the scan using the following criteria for the couplings and the soft parameters:

$$|\lambda_{T,S,TS}| \leq 1, \quad |\kappa| \leq 3, \quad |v_s| \leq 1 \text{ TeV}, \quad 1 \leq \tan\beta \leq 10,$$
$$|A_{T,S,TS,U,D}| \leq 1 \text{ GeV}, \quad |A_\kappa| \leq 3 \text{ GeV},$$
$$65 \leq |M_{1,2}| \leq 10^3 \text{ GeV}, \quad 3 \times 10^2 \leq m_{Q_3,\bar{u}_3,\bar{d}_3} \leq 10^3 \text{ GeV}.$$

$$(16)$$

We have selected those points which have one of the four Higgs bosons with a one-loop mass of ~ 125 GeV with one-loop minimization conditions and, out of the 1.35×10^6 points, over 10^5 of them pass this constraint. On this set of Higgs candidates, we have imposed the constraints on the structure of the lightest CP-even, CP-odd, and charged Higgses. The number of points with $h_1 \equiv h_{125}$ doubletlike and a_1 singletlike is about 70%, but we have just one point with $h_1 \equiv h_{125}$ which is doubletlike and a_1 tripletlike. If we add the requirement on the lightest charged Higgs to be tripletlike, we find that the number of points with $h_1 \equiv h_{125}$ doubletlike, a_1 singletlike, and $h_1^\pm$ tripletlike is 26%. The case of $h_2 \equiv h_{125}$ doubletlike allows more possibilities because, in this case, we have also to check the structure of h_1. However, we find 75 points only when h_1 is tripletlike, $h_2 \equiv h_{125}$ is doubletlike, and a_1 is singletlike. This selection is insensitive to the charged Higgs selection, i.e., we still have 75 points with h_1 tripletlike, $h_2 \equiv h_{125}$ doubletlike, a_1 singletlike, and $h_1^\pm$ tripletlike.

The LHC constraints have been imposed on those points with $h_1 \equiv h_{125}$ because they provide better statistics. For these points, we demand that

$$\mu_{WW^*} = 0.83 \pm 0.21 \quad \mu_{ZZ^*} = 1.00 \pm 0.29$$
$$\mu_{\gamma\gamma} = 1.12 \pm 0.24 \quad\quad (17)$$

at a 1σ confidence level [2]. The LHC selection gives us 12223 points out of the 26776 points that have $h_1 \equiv h_{125}$ doubletlike, a_1 singletlike, and $h_1^\pm$ tripletlike.

Apart from the LEP [17] and LHC [2] constraints, we also ensure the validity of the constraints coming from the B observables. For this particular reason, we claim the light pseudoscalar a_1 to be $\geq 90\%$ singlet type and the light charged Higgs $h_1^\pm$ to be 90% triplet type. A very light scalar or pseudoscalar, with a mass of around 1–10 GeV, gets strong bounds from bottomonium decay to $a_1\gamma$ [19]. The decay rate for $\Upsilon \rightarrow a_1\gamma$ can be approximated as follows:

$$\mathcal{B}(\Upsilon \rightarrow a_1\gamma) = \mathcal{B}(\Upsilon \rightarrow a_1\gamma)_{\text{SM}} \times g_{a_1 b\bar{b}}^2, \quad (18)$$

where $g_{a_1 b\bar{b}}$ is the reduced down-type Yukawa coupling with respect to the SM [20]. We checked explicitly that the requirement of more than 90% singlet type a_1 and low $\tan\beta$ ensures that we are in the region of validity.

Another important constraint for a light pseudoscalar comes from $\mathcal{B}(B_s \rightarrow \mu\mu)$, which can be summarized as follows [20]:

$$\mathcal{B}(B_s \rightarrow \mu\mu) \simeq \frac{2\tau_{B_s} M_{B_s}^5 f_{B_s}^2}{64\pi} |C|^2 (\mathcal{R}_{12}^P)^4, \quad (19)$$

with

$$C = \frac{G_F\alpha}{\sqrt{2}\pi} V_{tb} V_{ts}^* \frac{\tan^3\beta}{4\sin^2\theta_w} \frac{m_\mu m_t |\mu_r|}{m_W^2 (m_{a_1}^2 - m_{B_s}^2)} \frac{\sin 2\theta_{\tilde{t}}}{2} \Delta f_3,$$

$$(20)$$

where $\Delta f_3 = f_3(x_2) - f_3(x_1)$, $x_i = m_{\tilde{t}_i}^2/|\mu_r|^2$, $f_3(x) = x \ln x/(1-x)$, $\theta_{\tilde{t}}$ is the stop mixing angle, and $\mathcal{R}_{12}^P$ is the rotation angle, defined in Eq. (11), which gives the coupling with the down-type Higgs (H_d) with leptons and down-type quarks. The demand of mostly singlet a_1 ($\geq 90\%$) on the data set ensures that we are well below the current upper limit [21].

Another constraint that affects the models with an extra Higgs boson, especially the charged Higgs bosons, comes from the rare decay of $B \rightarrow X_s\gamma$. The charged Higgs bosons which are doublet in nature couple to quarks via Yukawa couplings and contribute to the rare decay of $B \rightarrow X_s\gamma$. Similar contributions also come from the charginos which couple to the quarks, namely, doublet-type Higgsinos and winos. However, when we have charged Higgs or charginos which are triplet in nature, they do not couple to the fermions and thus do not contribute to such decays [8,9]. If the light charged Higgs bosons are triplet in nature, the dominant Wilson coefficients $F_{7,8}$ are suppressed by the
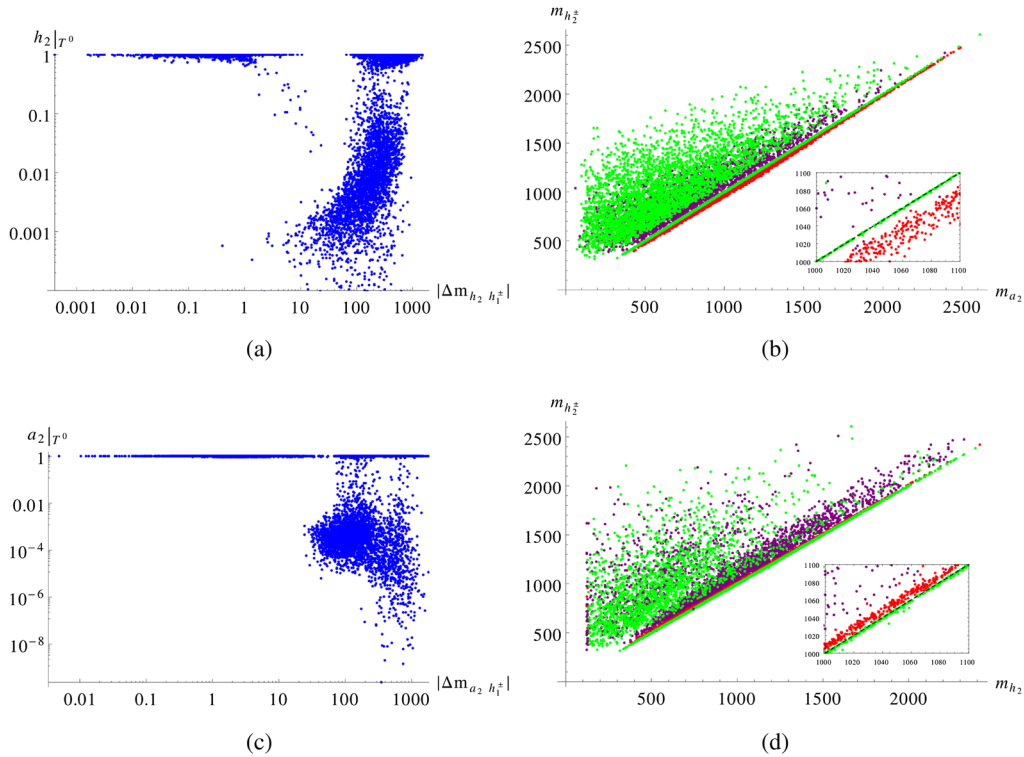
FIG. 1. We show the fraction of triplets of (a) h_2 and (c) a_2 as a function of the mass difference $|\Delta m_{h_2/a_2 h_1^\pm}|$ between h_2/a_2 and $h_1^\pm$, respectively. We plot the mass correlation (b) between a_2 and $h_2^\pm$ and (d) between h_2 and $h_2^\pm$. These exhaust the possible hierarchies for the triplet eigenstates. We mark in red the points with both a_2 and $h_2^\pm$ doublet type, in purple the points with a_2 triplet type, and $h_2^\pm$ doublet type, or vice versa, and in green the points with both a_2 and $h_2^\pm$ tripletlike.

charged Higgs rotation angles $\mathcal{R}_{11,13}^C$, as defined in Eq. (11). The demand of the light charged Higgs boson mostly triplet ($\geq 90\%$) enables us to avoid the constraint from $\mathcal{B}(B \to X_s\gamma)$ [8,9].

In Fig. 1(a), we plot the triplet fraction of h_2 in a function of the mass splitting between h_2 and $h_1^\pm$. The lightest charged Higgs is selected to be tripletlike ($\geq 90\%$). It is evident that, in the case of mass degeneracy between h_2 and $h_1^\pm$, the tripletlike structure of $h_1^\pm$ is imposed also on h_2. In Fig. 1(b), we plot the mass correlation between a_2 and $h_2^\pm$. We use the following color code: we mark in red the points with both a_2 and $h_2^\pm$ doublet type, in purple the points with a_2 triplet type and $h_2^\pm$ doublet type or vice versa, and in green the points with both a_2 and $h_2^\pm$ tripletlike. In the inset the dashed line indicates a configuration of mass degeneracy. It is evident that the mass degeneracy between a_2 and $h_2^\pm$ implies that both of them are tripletlike. As we depict in Fig. 2, there could be an exchange between a_2 and h_2 in the triplet pairs, shown in green. For this reason, we illustrate also the other possible hierarchy path in Figs. 1(c) and 1(d). As one may notice, the two sets of plots are qualitatively similar, although there is a quantitative difference between the red points of Figs. 1(b) and 1(d). The points in the latter are closer than the former to the line of mass degeneracy. Figure 3(a) shows that the more h_4 is decoupled compared to a_1, the more it tends to be in a singletlike eigenstate. We

remind that a_1 is a pseudo-Nambu-Goldstone (NG) mode, and hence it is naturally light. From Fig. 3(b) it is evident that h_4 takes the soft mass m_S coming from the singlet. Figure 4(a) shows the mass correlations between $h_3^\pm$ and a_3, while Fig. 4(b) shows the same correlation but between $h_3^\pm$, h_3, where all of them are of a doublet-type nature and are marked in red. It is easily seen that all three doubletlike Higgs bosons, $h_3^\pm$, h_3, and a_3, remain degenerate. There are
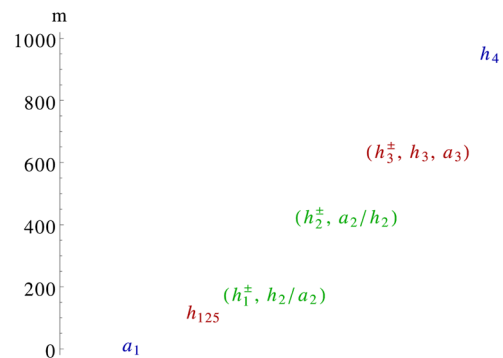

FIG. 2. A typical mass hierarchy of the scalar sector, with the singlet in blue, the doublets in red, and the triplet Higgs bosons in green. The eigenstates of the triplet sector with a_2/h_2 or h_2/a_2 are alternative: if $h_1^\pm$ pairs with the neutral h_2, then $h_2^\pm$ is mass degenerate with the pseudoscalar a_2 (and vice versa).
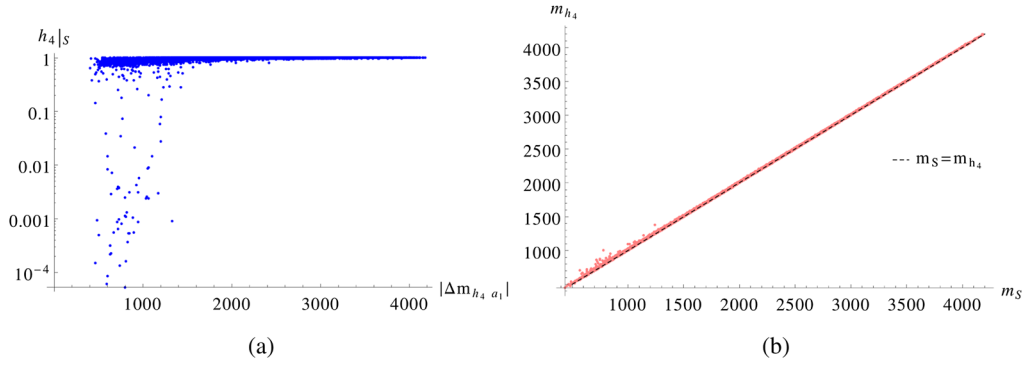
FIG. 3.   We show the singlet fraction of h_4 as a function of (a) the mass difference $|\Delta m_{h_4 a_1}|$ between the two states h_4 and a_1, and (b) the mass correlation between h_4 and m_S.
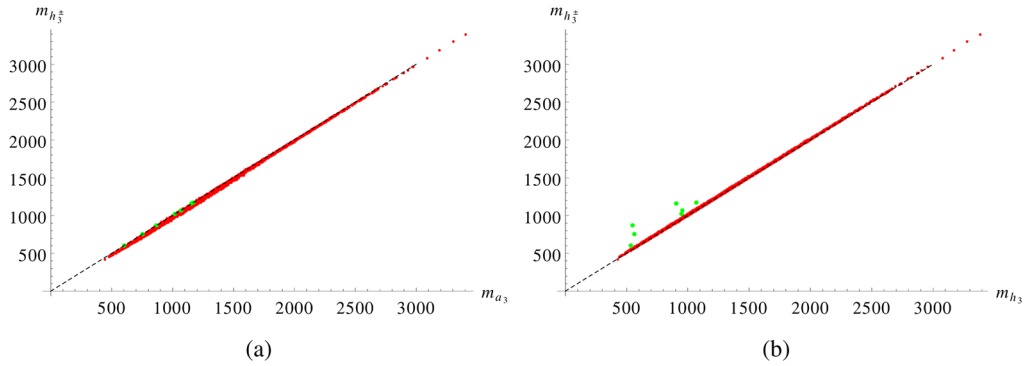

FIG. 4.   Scattered plots of the mass correlation (a) between a_3 and $h_3^{\pm}$ and (b) between h_3 and $h_3^{\pm}$. The color code is defined as follows: we mark in red the points where h_3, a_3, $h_3^{\pm}$ are mostly doublets ($\geq 90\%$), and in green the points where they are mostly triplet.

only seven points which behave like triplets and are shown in green. Thus, it is evident from the above analysis that eigenstates dominated by the same representation (i.e., mostly singlet or mostly triplet) tend to be hierarchically clustered. In the case of a Z_3 symmetric Lagrangian, the light pseudoscalar is actually a pseudo-NG mode of a continuous $U(1)$ symmetry of the Higgs potential, also known as the R axion [7], and remains very light across the entire allowed parameter space.

   Though the interaction eigenstates are a mixture of the gauge eigenstates, there seems to be a pattern for the various representations of the Higgs sector. A given representation tries to keep their masses in the same block, i.e., the masses of scalar, pseudoscalar, and charged components of the triplets will form a different mass block than the doublet Higgs sectors. A typical mass hierarchy is shown in Fig. 2, where a light pseudoscalar which is a pseudo-NG boson lies hidden below 100 GeV and the scalar state h_4 takes a heavy mass $\sim m_S$—and is therefore decoupled from the low energy spectrum. There is a CP-even Higgs boson of doublet type around 125 GeV and doubletlike heavy Higgs bosons of larger mass ($h_3^{\pm}$, h_3, a_3), shown in red. Apart from doublet and singlet interaction eigenstates, we have two triplets, T_1 and T_2, which then

form two different sets, ($h_1^{\pm}$, h_2/a_2) and ($h_2^{\pm}$, a_2/h_2), in the mass hierarchy, shown in green. Of course, this is not the most general situation, but it comes from the phenomenological constraints that should be applied to the scanned points in the parameter space. We remind the reader again that these constraints include a scalar Higgs boson with a mass of around 125 GeV, which satisfies the LHC constraint of Eq. (17), and no light doubletlike pseudoscalar or charged Higgs boson. We take care of the latter, requesting that the lightest pseudoscalar as mostly singlet and lightest charged Higgs boson is mostly triplet.

IV. CHARGED HIGGS BOSONS AND ITS STRUCTURE

   In this section we will describe the feature of the charged Higgs sector, emphasizing the role of the rotation angles in the limit $|\lambda_T| \simeq 0$. The charged Higgs bosons are a mixture of two doublet and two triplet fields, as can be seen from Eq. (21),

$$h_i^{\pm} = \mathcal{R}_{i1}^C H_u^+ + \mathcal{R}_{i2}^C T_2^+ + \mathcal{R}_{i3}^C H_d^{-*} + \mathcal{R}_{i4}^C T_1^{-*}, \quad (21)$$

with $\mathcal{R}_{i1,i3}^C$ and $\mathcal{R}_{i2,i4}^C$ determining the doublet and triplet parts, respectively. In general, $\mathcal{R}_{ij}^C$ is a function of all of the

VEVs, $\lambda_{T,TS,S}$, and the A_i parameters, and we can write schematically

$$\mathcal{R}_{ij}^C = f_{ij}^C(v_u, v_d, v_T, v_S, \lambda_T, \lambda_{TS}, \lambda_S, A_i). \qquad (22)$$

The charged Higgs mass matrix which is given in the Appendix [Eq. (A3)] shows a similar dependency on the parameters. However, the charged Goldstone mode, expressed in terms of the gauge eigenstates, is a function only of the VEVs and the gauge couplings, as we expect from the Goldstone theorem:

$$h_0^\pm = \pm N_T \left(\sin\beta H_u^+ - \cos\beta H_d^{-*} \mp \sqrt{2}\frac{v_T}{v}(T_2^+ + T_1^{-*}) \right)$$

$$N_T = \frac{1}{\sqrt{1 + 4\frac{v_T^2}{v^2}}}. \qquad (23)$$

Equation (23) presents the explicit expression of the charged Goldstone mode, and we can see that it is independent of any other kind of coupling or parameter. Among the three kinds of VEVs entering in the charged Goldstone mode, the triplet VEV is very small ($v_T \lesssim 5$ GeV) due to its contribution to the $W^\pm$ boson mass, as was discussed in Eq. (8). The triplet VEV, being restricted by the ρ parameter [18], makes the charged Goldstone always doublet type. However, among the massive states in the gauge basis, two of them are tripletlike and one is doubletlike. We shall see later that this small triplet contribution to the Goldstone boson protects one of the three physical charged Higgs bosons from becoming absolute tripletlike.

In Fig. 5 we show the structure of the charged Higgs bosons as a function of $|\lambda_T|$, where we demand the lightest charged Higgs massive state to be mostly triplet. One can realize that, for a nonzero λ_T, their tendency is to mix. However, as we move towards the $|\lambda_T| \simeq 0$ region, one of the charged Higgs bosons gives away the $\sim(\frac{v_T}{v})^2$ triplet part to the charged Goldstone and fails to become 100% triplet (see the blue points in Fig. 5). In the models where the A_T parameter is proportional to λ_T, the mixing induced by the soft parameter A_T automatically goes to zero in this limit. However, the mixing of doublet and triplet in the charged Goldstone comes from the corresponding VEVs and is independent of λ_T or A_T, as can be seen from Eq. (21). Now all of the other massive charged Higgs bosons are orthogonal to the Goldstone boson, which makes a similar mixing in the massive states as well. This mixing goes to zero only when the triplet does not play any role in EWSB, i.e., $v_T = 0$. However, for nonzero λ_T's and A_T's, the additional mixings come for the massive eigenstates.

Any one of the three massive charged Higgs boson can show this feature, but we see it only for $h_1^\pm$ because in the selection criteria we have demanded that $h_1^\pm$ must be tripletlike. Thus, for a nonzero triplet VEV, even with $|\lambda_T| = 0$, complete decoupling of doublet and triplet
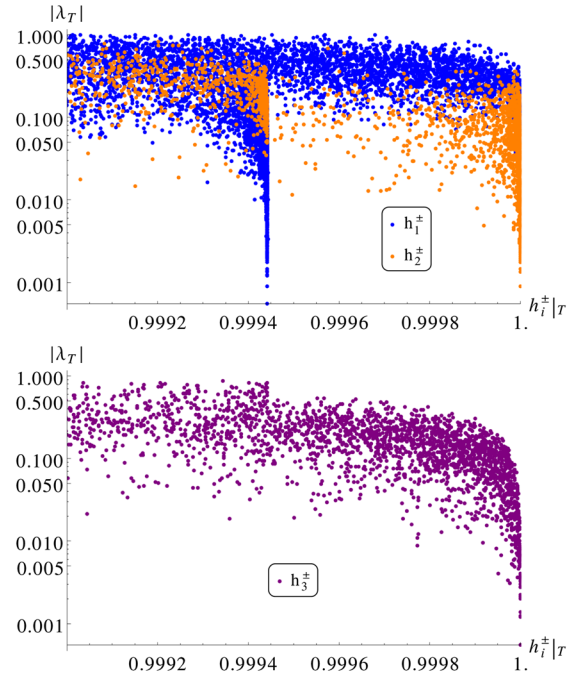

FIG. 5. Triplet component of the massive charged Higgs bosons versus λ_T.

representations is not possible. Therefore by "decoupling limit" we mean $|\lambda_T| \simeq 0$ here onwards. In this decoupling limit, either the $h_2^\pm$ or the $h_3^\pm$ become completely of triplet type. A similar conclusion was shown for the triplet extension of the supersymmetric Standard Model [12].

The decoupling limit of $|\lambda_T| \sim 0$ affects not only the structure of the charged Higgs bosons, where two of them become tripletlike and one of them doubletlike, but also the respective coupling via the corresponding rotation angles. In Fig. 6 we show the rotation matrix elements for the light charged Higgs boson $h_1^\pm$ with respect to $|\lambda_T|$. We can see that, when λ_T becomes very small, the mixing angles in the triplet component of the light charged Higgs boson $h_1^\pm$, $\mathcal{R}_{12}^C$, and $\mathcal{R}_{14}^C$, as defined in Eq. (21), take the same signs, unlike in the general case. We will see later that the presence of the same signs in $\mathcal{R}_{12}^C$ and $\mathcal{R}_{14}^C$ in the decoupling limit causes an enhancement of some production channels and a decrement for some other ones.

V. DECAYS OF THE CHARGED HIGGS BOSONS

As briefly mentioned above, the phenomenology of the Higgs decay sector of the TNMSSM, as discussed in [13], is affected by the presence of a light pseudoscalar which induces new decay modes. In this section we consider its impact in the decay of a light charged Higgs boson, $h_1^\pm$. Along with the existence of the light pseudoscalar, which opens up the $h_1^\pm \to a_1 W^\pm$ decay mode, the tripletlike charged Higgs adds new decay modes, not possible otherwise. In particular, a $Y = 0$ tripletlike charged
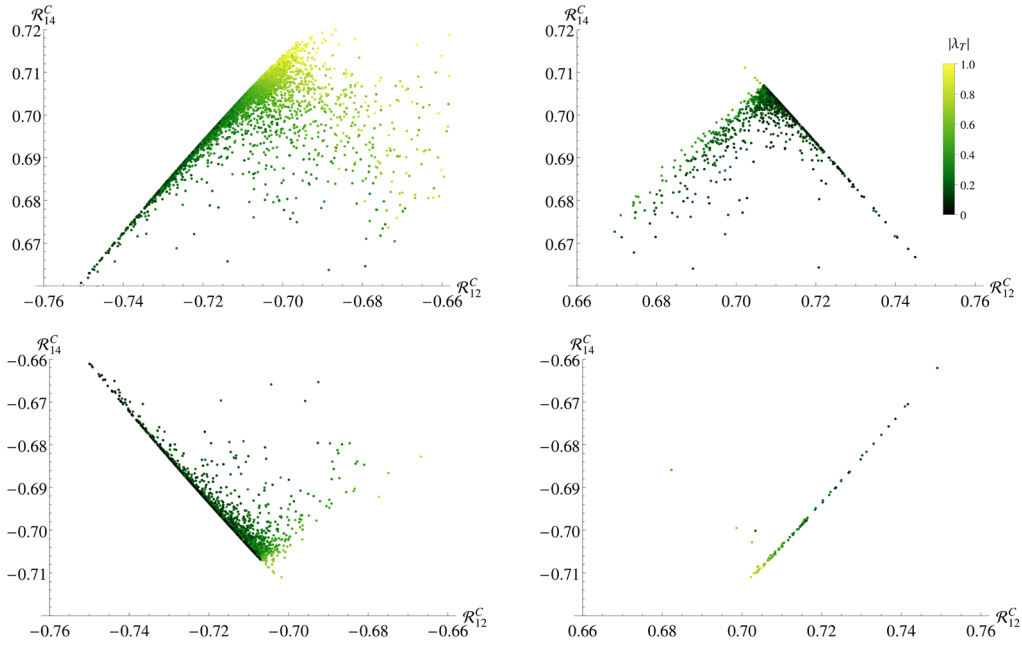
FIG. 6.   Correlations of the rotation angles of the lightest charged Higgs boson $h_1^\pm$ as a function of λ_T.

Higgs boson gets a new decay mode into $ZW^\pm$, which is a signature of custodial symmetry breaking. Apart from that, the usual doubletlike decay modes into $\tau\nu$ and tb are present via the mixings with the doublets.

A. $h_i^\pm \to W^\pm h_j/a_i$

The trilinear couplings with charged Higgses, scalar (pseudoscalar) Higgses, and $W^\pm$ are given by

$$g_{h_i^\pm W^\mp h_j} = \frac{i}{2} g_L (\mathcal{R}_{j2}^S \mathcal{R}_{i3}^C - \mathcal{R}_{j1}^S \mathcal{R}_{i1}^C + \sqrt{2}\mathcal{R}_{j4}^S (\mathcal{R}_{i2}^C + \mathcal{R}_{i4}^C)),$$
(24)

$$g_{h_i^\pm W^\mp a_j} = \frac{g_L}{2} (\mathcal{R}_{j1}^P \mathcal{R}_{i1}^C + \mathcal{R}_{j2}^P \mathcal{R}_{i3}^C + \sqrt{2}\mathcal{R}_{j4}^P (\mathcal{R}_{i2}^C - \mathcal{R}_{i4}^C)).$$
(25)

Both the triplet and doublet has $SU(2)$ charges so they couple to $W^\pm$ boson. Their coupling associated with neutral Higgs bosons have to be doublet (triplet) type for doublet- (triplet-) type charged Higgs bosons. For the phenomenological studies, we have considered a doubletlike Higgs boson of around 125 GeV, a light tripletlike charged Higgs boson $\lesssim 200$ GeV and a very light singlet-type pseudoscalar of ~ 20 GeV. Hence, the mixing angles become really important. In the next few sections, we will see how the various rotation angles involved with the charged Higgs bosons and their relative signs determine the strength of the couplings, and thus of the decay widths. Equation (24) shows that, for a $h_i^\pm \to W^\pm h_j$ decay, the rotation angles $\mathcal{R}_{i2}^C$

and $\mathcal{R}_{i4}^C$ display as additive, whereas for $h_i^\pm \to W^\pm a_j$ they display as subtractive.

The decay width of a massive charged Higgs boson in a W boson and a scalar (or pseudoscalar) boson is given by

$$\Gamma_{h_i^\pm \to W^\pm h_j/a_j} = \frac{G_F}{8\sqrt{2}\pi} m_{W^\pm}^2 |g_{h_i^\pm W^\mp h_j/a_j}|^2$$
$$\times \sqrt{\lambda(1, x_W, x_{h_j/a_j})} \lambda(1, y_{h_i^\pm}, y_{h_j/a_j}),$$
(26)

where $x_{W,h_j} = \frac{m_{W,h_j}^2}{m_{h_i^\pm}^2}$ and $y_{h_i^\pm,h_j} = \frac{m_{h_i^\pm,h_j}^2}{m_{W^\pm}^2}$, and similarly for a_j.

Figure 7 shows the dependency of the $g_{h_1^\pm W^\mp a_1}$ coupling with the triplet components of the lightest charged Higgs
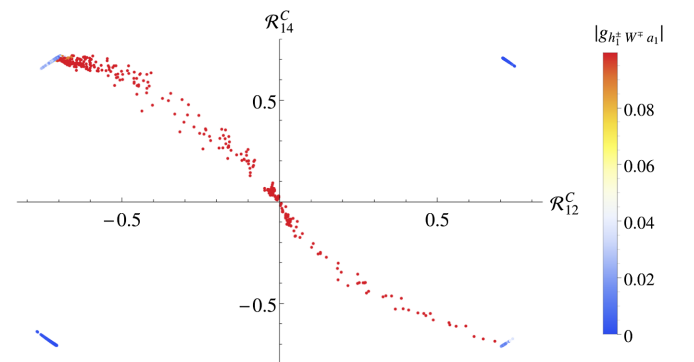

FIG. 7.   Correlation of $g_{h_i^\pm W^\mp a_1}$ with $\mathcal{R}_{12}^C$ and $\mathcal{R}_{14}^C$. For the blue points in quadrants II and IV, the low values of the coupling are due to the selection of a singletlike a_1, which means that $\mathcal{R}_{13}^P \sim 1$, whereas, for the blue points in quadrants I and III, the low value of $|g_{h_1^\pm W^\mp a_1}|$ comes from the cancellation between $\mathcal{R}_{12}^C$ and $\mathcal{R}_{14}^C$.

TABLE I.   The sign of the product $\mathcal{R}_{12}^C \mathcal{R}_{14}^C$. The sign of the two rotation angles of the lightest charged Higgs boson plays a crucial role in the interactions of a tripletlike charged Higgs boson. In the limit $|\lambda_T| \sim 0$, these two rotation angles have the same sign. This feature has important consequences for the interaction, and hence the cross section, of the lightest charged Higgs boson in various channels.

	$10^{-2} < |\lambda_T| < 1$	$|\lambda_T| < 10^{-2}$
sign $\mathcal{R}_{12}^C \mathcal{R}_{14}^C$	$+$ or $-$	$+$

eigenstate, i.e., $\mathcal{R}_{12}^C$ and $\mathcal{R}_{14}^C$. We have seen from Fig. 6 and Table I the behavior of $\mathcal{R}_{12}^C \mathcal{R}_{14}^C$ as a function of λ_T, i.e., that for $\lambda_T \sim 0$ they take the same sign. We can see that, in the decoupling limit, i.e., for $\lambda_T \sim 0$, the coupling decreases because $\mathcal{R}_{12}^C$ and $\mathcal{R}_{14}^C$ take the same sign and they tend to cancel; cf. Eq. (24). A low value of this coupling can come even when the pseudoscalar Higgs boson (a_j) is singletlike, which means that $\mathcal{R}_{j3}^P \sim 1$. The situation is just the opposite in the case of $g_{h_1^\pm W^\mp h_1}$, as one can see from Fig. 8. Here, in the decoupling limit, the coupling $g_{h_1^\pm W^\mp h_1}$ is enhanced. In Fig. 8 we can also see some blue points with low $\mathcal{R}_{12}^C$, $\mathcal{R}_{14}^C$. In this case the charged Higgs boson is not tripletlike and the suppression in the coupling is due to the accidental cancellation of $(\mathcal{R}_{12}^S \mathcal{R}_{13}^S - \mathcal{R}_{11}^S \mathcal{R}_{11}^S)$; cf. Eq. (24). This cancellation is, of course, not related to the limit $\lambda_T \sim 0$. We see later how it affects the corresponding production processes.

B. $h_i^\pm \to W^\pm Z$

The charged sector of a theory with scalar triplet(s) is very interesting due to the tree-level interactions $h_i^\pm - W^\mp - Z$ for $Y = 0, \pm 2$ hypercharge triplets, which break the custodial symmetry [11,12,15,16]. In the TNMSSM, this coupling is given by
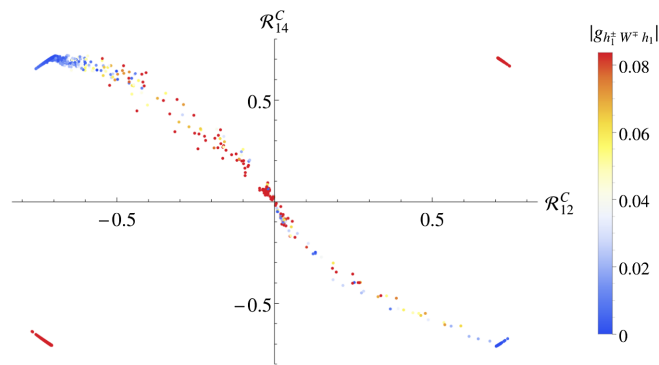
$$g_{h_i^\pm W^\mp Z} = -\frac{i}{2}(g_L g_Y (v_u \sin\beta \mathcal{R}_{i1}^C - v_d \cos\beta \mathcal{R}_{i3}^C)$$
$$+ \sqrt{2} g_L^2 v_T (\mathcal{R}_{i2}^C + \mathcal{R}_{i4}^C)), \qquad (27)$$

where the rotation angles are defined in Eq. (11). The on-shell decay width is given by

$$\Gamma_{h_i^\pm \to W^\pm Z} = \frac{G_F \cos^2\theta_W}{8\sqrt{2}\pi} m_{h_i^\pm}^3 |g_{h_i^\pm W^\mp Z}|^2$$
$$\times \sqrt{\lambda(1, x_W, x_Z)}(8 x_W x_Z + (1 - x_W - x_Z)^2), \qquad (28)$$

where $\lambda(x, y, z) = (x - y - z)^2 - 4yz$ and $x_{Z,W} = \frac{m_{Z,W}^2}{m_{h_i^\pm}^2}$ [22].

Figure 9 shows the dependency of $g_{h_i^\pm W^\mp Z}$ with respect to $\mathcal{R}_{12}^C$ and $\mathcal{R}_{14}^C$. We see that, for $\lambda_T \sim 0$, $\mathcal{R}_{12}^C$ and $\mathcal{R}_{14}^C$ take the same sign, and hence the $h_i^\pm - W^\mp - Z$ coupling is enhanced.

C. $h_i^\pm \to tb$

Besides the nonzero $h_i^\pm - W^\mp - Z$ coupling at tree level due to custodial symmetry breaking, the charged Higgs bosons can also decay into fermions through the Yukawa interaction given below:

$$g_{h_i^+ \bar{u} d} = i(y_u \mathcal{R}_{i1}^C \mathsf{P}_\mathsf{L} + y_d \mathcal{R}_{i3}^C \mathsf{P}_\mathsf{R}), \qquad (29)$$

governed by the doublet part of the charged Higgses. The decay width at leading order is

$$\Gamma_{h_i^\pm \to ud} = \frac{3}{4} \frac{G_F}{\sqrt{2}\pi} m_{h_i^\pm} \sqrt{\lambda(1, x_u, x_d)} \left[(1 - x_u - x_d) \right.$$
$$\times \left(\frac{m_u^2}{\sin^2\beta}(\mathcal{R}_{i1}^C)^2 + \frac{m_d^2}{\cos^2\beta}(\mathcal{R}_{i3}^C)^2 \right)$$
$$\left. - 4 \frac{m_u^2 m_d^2}{m_{h_i^\pm}^2} \frac{\mathcal{R}_{i1}^C \mathcal{R}_{i3}^C}{\sin\beta \cos\beta} \right], \qquad (30)$$
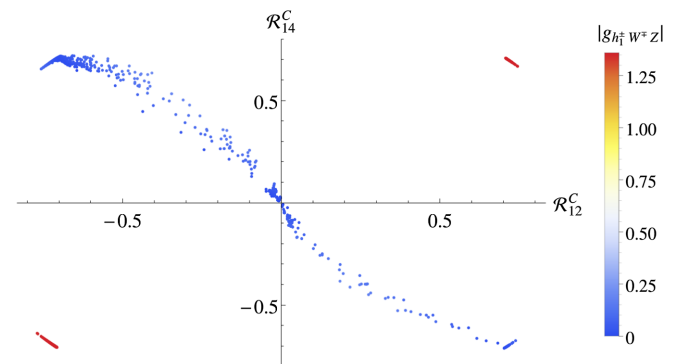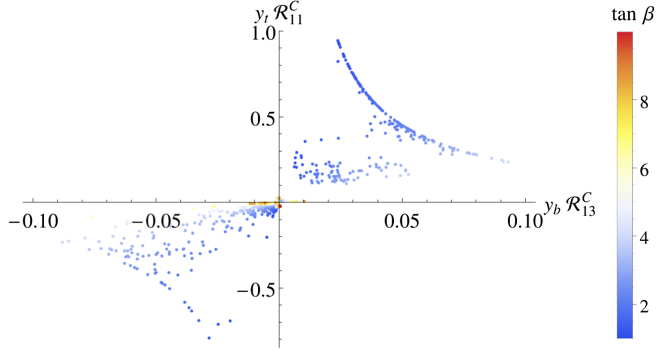

FIG. 8.   Correlation of $g_{h_1^\pm W^\mp h_1}$ with $\mathcal{R}_{12}^C$ and $\mathcal{R}_{14}^C$. The coupling is enhanced when $\mathcal{R}_{12}^C$ and $\mathcal{R}_{14}^C$ are small, i.e., for a doubletlike charged Higgs $h_1^\pm$. The enhancement in quadrants I and III are related to the same sign of $\mathcal{R}_{12}^C$ and $\mathcal{R}_{14}^C$; cf. Eq. (24).

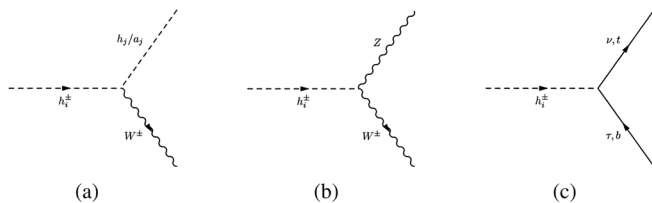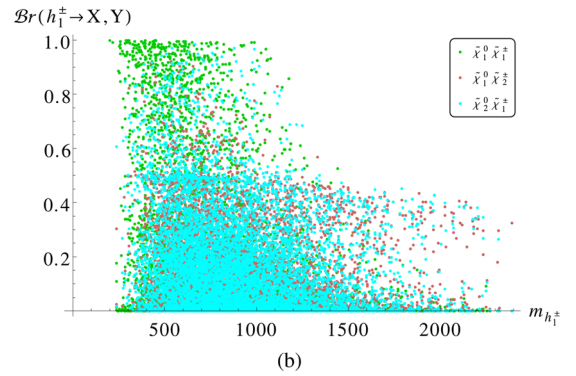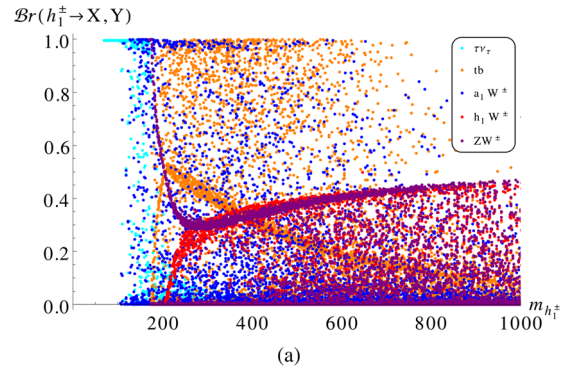FIG. 9.   Correlation of $g_{h_1^\pm W^\mp Z}$ with $\mathcal{R}_{12}^C$ and $\mathcal{R}_{14}^C$.

FIG. 10. Correlation of $y_t \mathcal{R}_{11}^C$ and $y_b \mathcal{R}_{13}^C$ as a function of $\tan \beta$.

where $x_{u,d} = \frac{m_{u,d}^2}{m_{h_i^\pm}^2}$. The QCD correction to the leading order formula are the same as in the MSSM and are given in [23]. The decay of the charged Higgs bosons into quarks is then suppressed in the case of tripletlike eigenstates, as one can easily realize from the expression above. In Fig. 10 we show the correlation of the effective Yukawa coupling ($y_u \mathcal{R}_{i1}^C$ and $y_d \mathcal{R}_{i3}^C$) of the top and bottom quarks, respectively, as a function of $\tan \beta$. The dominant contribution comes from the top for a small $\tan \beta$, as we expected.

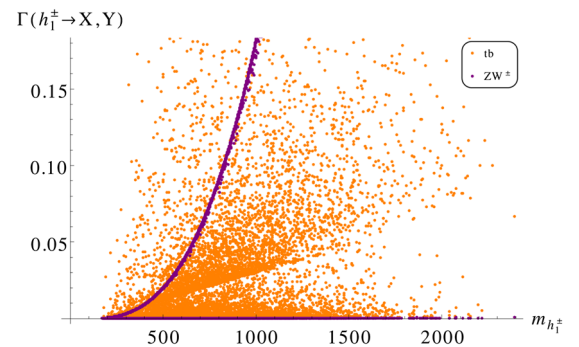## VI. DECAY BRANCHING RATIOS OF THE CHARGED HIGGS BOSONS

Prepared with the possibilities of new decay modes, we finally analyze such scenarios with the data satisfying various theoretical and experimental constraints. The points here have a CP-even neutral Higgs boson around 125 GeV which satisfies the LHC constraint given in Eq. (17). To study the decay modes and calculate the branching fractions, we have implemented our model in SARAH4.4.6 [24] and we have generated the model files for CalcHEP3.6.25 [25].

Figure 11(a–c) describes the main decay modes for the charged Higgs bosons and Fig. 12(a) presents the decay branching ratios of the light charged Higgs boson $h_1^\pm$ into nonsupersymmetric modes. This includes the $a_1 W^\pm$, $h_1 W^\pm$, $ZW^\pm$, tb, and $\tau\nu$ channels. The points in Fig. 12 include a discovered Higgs boson at ~ 125 GeV and a tripletlike light charged Higgs boson $h_i^\pm$. When a_1 is singlet type, the $a_1 W^\pm$ decay mode is suppressed, despite being

FIG. 12. The branching ratios for the decay of the lightest charged Higgs boson $h_1^\pm$ into (a) nonsupersymmetric and (b) supersymmetric modes.

kinematically open. One can notice that, with the $h_1^\pm$ being tripletlike, the decay mode $ZW^\pm$ can be very large, even close to 100%. When the tb mode is kinematically open, the $ZW^\pm$ gets an apparent suppression, but it increases again for a charged Higgs bosons of larger mass ($m_{h_i^\pm} \sim 400$ GeV). This takes place because the $h_i^\pm \to ZW^\pm$ decay width is proportional to $m_{h_i^\pm}^3$, unlike the tb one, which is proportional to $m_{h_i^\pm}$ [see Eqs. (28) and (30)]. The variation of these two decay widths, as a function of $m_{h_1^\pm}$, is shown in Fig. 13.

Figure 12(b) shows the decays of the lightest charged Higgs boson into the supersymmetric modes, i.e., into

FIG. 11. Figures (a–c) describe the decay of the charged Higgs boson in $h_j/a_j W^\pm$, $ZW^\pm$ and ν/b, τ/t respectively.

FIG. 13. The decay widths of the lightest charged Higgs boson $h_1^\pm$ to tb and $ZW^\pm$.
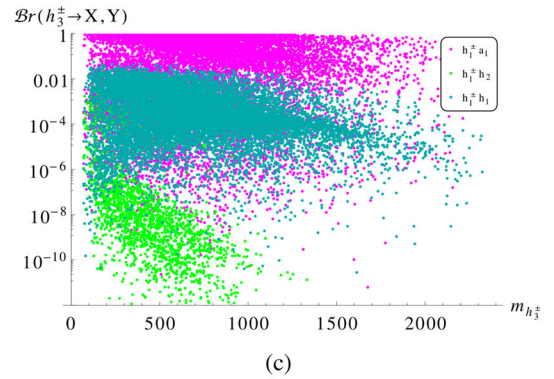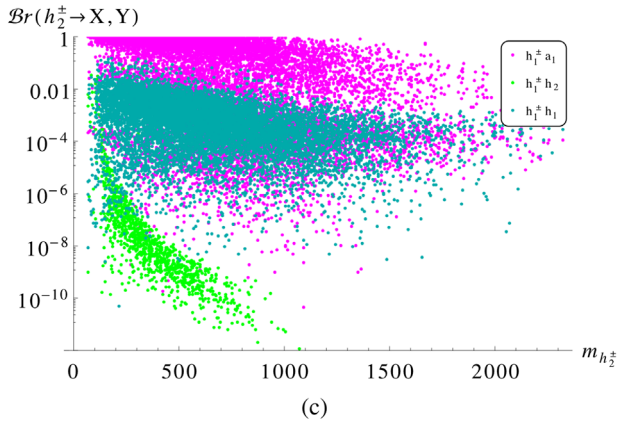
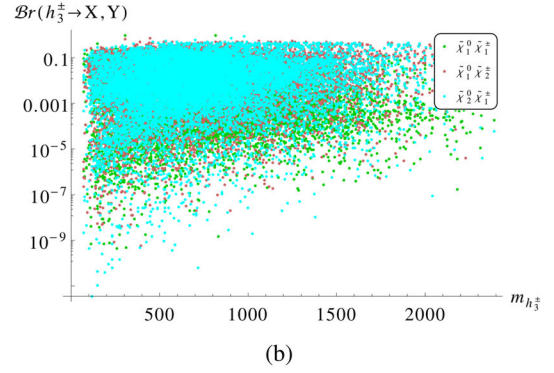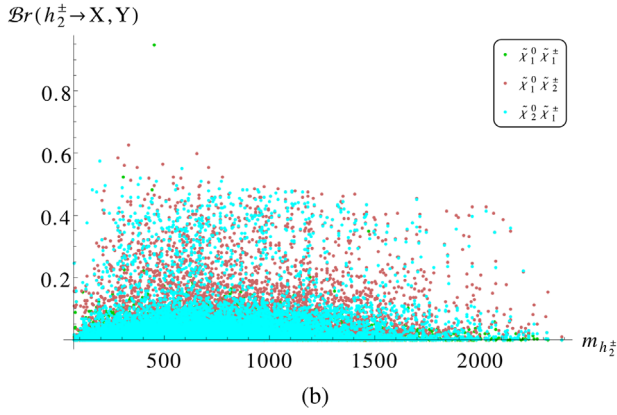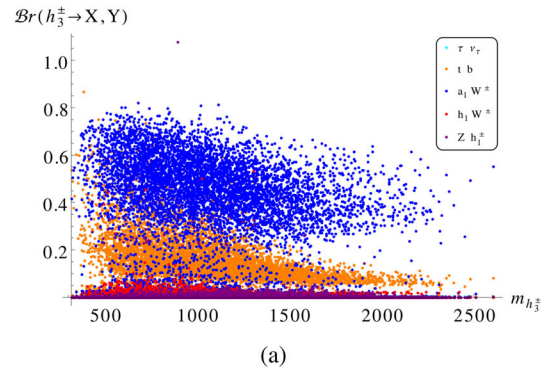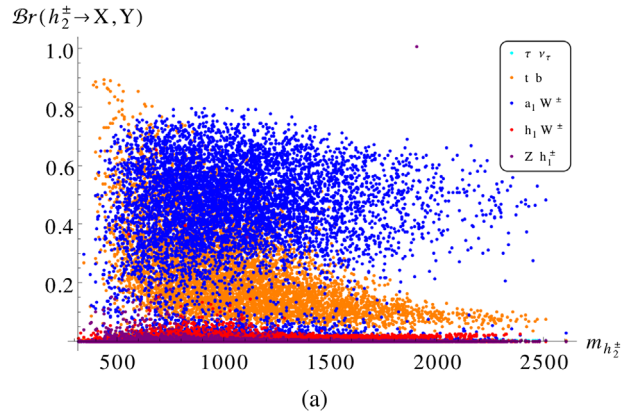FIG. 14.   The branching ratios of the decay of the charged Higgs boson $h_2^\pm$ into (a) nonsupersymmetric and (b) supersymmetric modes, and (c) into Higgs bosons.

charginos $\tilde{\chi}_i^\pm$ and neutralinos $\tilde{\chi}_j^0$, when these modes are kinematically allowed. We observe that, for a charged Higgs boson of a relatively higher mass $m_{h_i^\pm} \gtrsim 300$ GeV, these modes open up and can have very large branching ratios.

Apart from the lightest charged Higgs boson, there are two additional charged Higgs bosons, $h_2^\pm$ and $h_3^\pm$. As we have pointed out many times, we have selected data points for which the light charged Higgs boson is triplet type. Certainly, in the decoupling limit, i.e., when $|\lambda_T| \simeq 0$, one of either $h_{2,3}^\pm$ is tripletlike, and the other one is doubletlike.
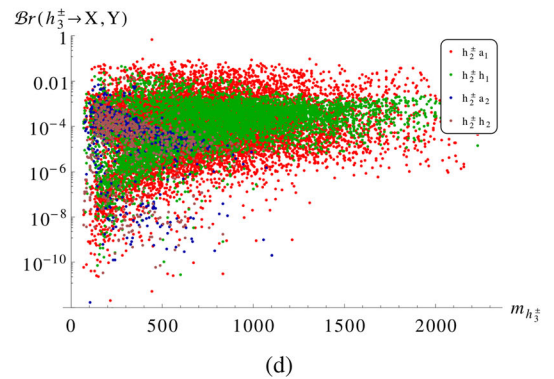

FIG. 15.   The branching ratios of the decay of the charged Higgs boson $h_3^\pm$ into (a) nonsupersymmetric and (b) supersymmetric modes, (c) the lightest charged Higgs boson $h_1^\pm$ associated with the neutral Higgs bosons, and (d) a second light charged Higgs boson $h_2^\pm$ associated with the neutral Higgs bosons.

The points that we have generated, which also satisfy the precondition of allowing an h_{125} in the spectrum, have an $h_2^\pm$ as a tripletlike and an $h_3^\pm$ as a doubletlike Higgs boson; cf. Fig. 5. In Fig. 14 we present the decay branching ratios of the second charged Higgs boson $h_2^\pm$. Figure 14(a) shows the ratios in $\tau\nu$, tb, $a_1 W^\pm$, $h_1 W^\pm$, and $Z h_1^\pm$. As one can observe, tb and $a_1 W^\pm$ are the dominant modes reaching up to $\sim 90\%$ and $\sim 80\%$, respectively. Figure 14(b) shows the branching ratios into supersymmetric modes with neutralinos and charginos, which are kinematically allowed. For some benchmark points, these modes can have decay ratios as large as $\sim 60\%$. Figure 14(c) shows the ratios for $h_2^\pm$ decaying into two scalars, i.e., to $h_1^\pm h_{1,2}$ and $h_1^\pm a_1$, with the $h_1^\pm a_1$ final state being the dominant among all.

Figure 15 presents the third charged Higgs boson $h_3^\pm$ decays. From Fig. 15(a) we can see that, for a large parameter space, the decay branching fraction to $a_1 W^\pm$ is the most relevant mode which can be probed at the LHC, even though tb mode is kinematically open but not the most dominant one. Figure 15(b) shows that the $\tilde{\chi}_2^0 \tilde{\chi}_1^\pm$ mode is kinematically open and also one of the most important. Figure 15(c) shows the decay branching ratios for the decay modes into the lightest charged Higgs boson associated with the neutral Higgs bosons. It is evident that the $h_1^\pm a_1$ mode is the most important, and one can probe more than one charged Higgs boson and also the light pseudoscalar. In Fig. 15(d) the branching ratios are shown where the heaviest charged Higgs boson $h_3^\pm$ decays to the second lightest charged Higgs boson $h_2^\pm$ associated with the neutral Higgs bosons. Again, the light pseudoscalar mode can have large branching ratios.

VII. PRODUCTION CHANNELS OF A LIGHT CHARGED HIGGS BOSON

The triplet nature of the charged Higgs bosons adds a few new production processes at the LHC alongside the doubletlike charged Higgs production process. For a doubletlike charged Higgs boson, the production processes are dominated by the top quark decay for the light charged Higgs boson ($m_{h_i^\pm} < m_t$), or $bg \to t h_i^\pm$ for ($m_{h_i^\pm} > m_t$), which are governed by the corresponding Yukawa coupling and $\tan\beta$, viz., in the two Higgs doublet model (2HDM), the MSSM, and the NMSSM. In the TNMSSM, however, the charged Higgs bosons can be tripletlike, and hence they do not couple to fermions. Fermionic channels, including top and bottom and, in general, all fermions, are then suppressed. The presence of the $h_i^\pm - W^\mp - Z$ vertex generates new production channels and also modifies the known processes for the production of a charged Higgs boson $h_i^\pm$. In these sections we address the dominant and characteristically different production mechanisms for the light charged Higgs bosons $h_1^\pm$ at the LHC. For this purpose, we select in the parameter space the benchmark points with a discovered Higgs boson of around 125 GeV and with the lightest charged Higgs boson $h_1^\pm$ that is
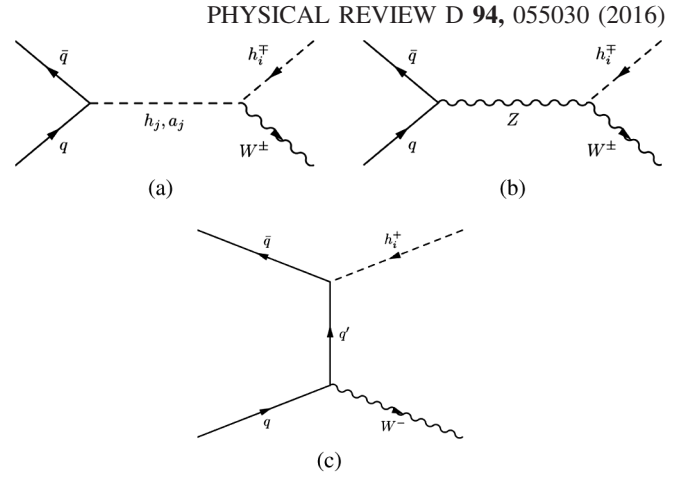

FIG. 16. Figures (a–c) describe the production of charged Higgs boson in association with $W^\pm$ boson via h_j/a_j, Z and q' exchange respectively.

tripletlike ($\geq 90\%$). The cross sections are calculated at the LHC with a center of mass energy of 14 TeV for such events. We have performed our analysis at leading order, using CalcHEP3.6.25 [25], using the CTEQ6L [26] set of parton distributions and a renormalization/factorization scale $Q = \sqrt{\hat{s}}$, where $\hat{s}$ denotes the total center of mass energy squared at parton level.

A. Associated $W^\pm$

The dominant channels are shown in Fig. 16, which are mediated by the neutral Higgs bosons, the Z boson, and the quarks. Figure 16(b), which describes the Z mediation, requires the nonzero $h_1^\pm - W^\mp - Z$ vertex, which is absent in theories without the $Y = 0, \pm 2$ triplet-extended Higgs sector. For a doubletlike charged Higgs, the only contributions come from the neutral Higgs-mediated diagrams in the s-channel and t-quark mediated diagram in the t-channel [see Figs. 16(a) and 16(c)]. For a low $\tan\beta$ case, the t-channel contribution in $b\bar{b}$ fusion is really large due to large Yukawa coupling. We will see that this admixture of the doublet still affects the production cross section at low $\tan\beta$.

The contribution of h_1 is subdominant because h_1 and $h_1^\pm$ are selected to be mostly doublet and mostly triplet, respectively, in order to satisfy the LHC data. The coupling of a totally triplet charged Higgs boson with a totally doublet neutral Higgs boson and a W boson is not allowed by gauge invariance. For the lightest tripletlike charged Higgs boson, one of the degenerate neutral Higgs bosons, either h_2 or a_2, is also tripletlike and fails to contribute as mediator in the $b\bar{b}$ fusion mode [Fig. 16(a)]. The other relevant neutral Higgs boson which is not degenerate with the lightest charged Higgs boson, $h_1^\pm$, contributes to the $b\bar{b}$ fusion production process via its doublet mixings. Thus, doublet-triplet mixing part plays an important role—even when we are trying to produce a light charged Higgs boson which is tripletlike. This feature also has been observed in
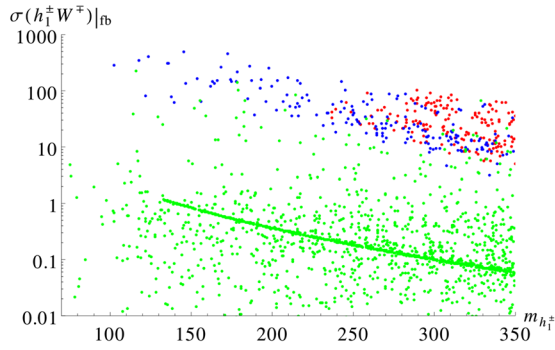
FIG. 17. The production cross section of $h_1^\pm W^\mp$ at the LHC versus the lightest charged Higgs boson mass, $m_{h_1^\pm}$. The red ones are $\geq 90\%$ doubletlike, the green ones are $\geq 90\%$ tripletlike, and the blue ones are mixed-type light charged Higgs bosons.

FIG. 19. The production cross section of the light charged Higgs boson $h_1^\pm$ associated with the Z boson versus the light charged Higgs boson mass $m_{h_1^\pm}$.

the triplet extended supersymmetric Standard Model (TESSM) [11]. Even the off-shell doublet-type neutral Higgs mediation (h_{125}) in the s-channel via gluon-gluon fusion fails to give sufficient contribution to the $h_1^\pm W^\mp$ final state. We checked to see that such a process at the LHC for a center of mass energy of 14 TeV and a tripletlike charged Higgs of a mass of $\sim$300 GeV and an $h_1^\pm W^\mp$ cross section is below $\mathcal{O}(10^{-3})$ fb.

In Fig. 17 we present the associated production cross section for a light charged Higgs boson $h_1^\pm$, together with the light charged Higgs boson mass $m_{h_1^\pm}$. The red ones are $\geq$90% doubletlike, the green ones are $\geq$90% tripletlike, and blue ones are mixed-type light charged Higgs bosons. It can be seen that, as the doublet fraction grows, the production cross section also grows. At $\lambda_T \simeq 0$, the lightest charged Higgs cannot be completely tripletlike due to the doublet fraction $\frac{v_T}{v}$. In this limit the cross section follows the line given by the green points in Fig. 17. As we saw in the previous section, for $\lambda_T \neq 0$ the coupling $g_{h_1^\pm W^\mp Z}$ is very small, even if the lightest charged Higgs is completely tripletlike. This means that the Z propagator [cf. Fig. 16(b)] does not make a contribution. However, since, for $\lambda_T \neq 0$, the triplet fraction of $h_1^\pm$ is not fixed, the cross section can be enhanced or decreased compared to the $|\lambda_T| \simeq 0$ one.

B. Associated Z

Unlike the previous case, the charged Higgs production associated with Z does not have sizable contributions from the doublet part of the Higgs boson spectrum. For instance, the doublet nature of the charged Higgs allows its exchange in the s-channel, as shown in Fig. 18(a), via an annihilation process ($q\bar{q}'$) which requires quarks of different flavors. The contributions from the valence $u/\bar{d}$, $\bar{u}/d$ distributions in a pp collision are strongly suppressed by the much lower Yukawa couplings. On the other hand, contributions from heavier generations such as $c/\bar{b}$, $\bar{c}/b$ are suppressed by Cabibbo-Kobayashi-Maskawa (CKM) mixing angles and the involvement of sea quarks in the initial state.

Nevertheless, in the case of the TNMSSM, a nonzero $h_1^\pm - W^\mp - Z$ vertex gives an extra contribution to this production process which is absent in the case of doublet-like charged Higgs bosons. In fact, for $\lambda_T \simeq 0$, which corresponds to what we have called the decoupling limit, the T_1^+ and T_2^- interaction eigenstates contribute additively to the $h_1^\pm - W^\mp - Z$ vertex, as can be seen from Eq. (27) and can also be realized from viewing Figs. 6 and 9. However, we can see from Fig. 19 that the $h_1^\pm Z$ production cross section is smaller than the respective production associated with a $W^\pm$. This is due to the fact that there are no other efficient contributions besides the channel with the $W^\pm$ in the propagator, as discussed earlier.

C. Associated h_1

We have considered, then, the production of the charged Higgs boson production associated with a scalar Higgs boson, h_i. It is clear from Fig. 20 that there are two contributions to this channel, one via the doublet-type

(a)   (b)
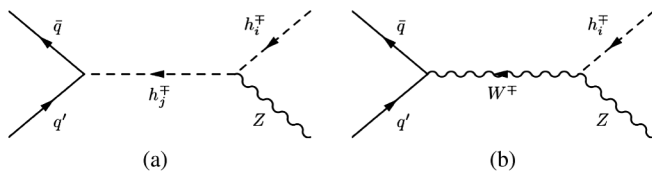
FIG. 18. Figures (a,b) describe the production of charged Higgs boson in association with Z boson via $h_j^\pm$ and $W^\pm$ boson exchange.

(a)   (b)

FIG. 20. Figures (a,b) describe the production of charged Higgs boson in association with h_i boson via $h_k^\pm$ and $W^\pm$ boson exchange.

FIG. 21. The production cross section of a light charged Higgs boson, $h_1^\pm$, associated with the h_1 boson versus the light charged Higgs boson mass $m_{h_1^\pm}$.
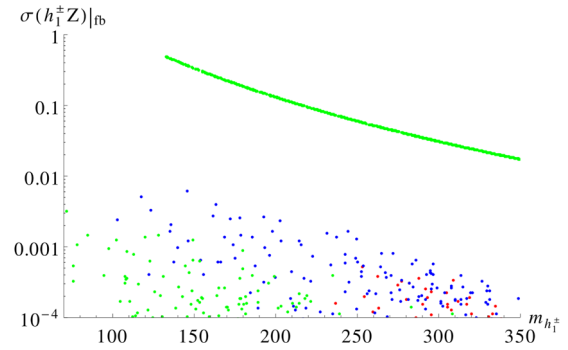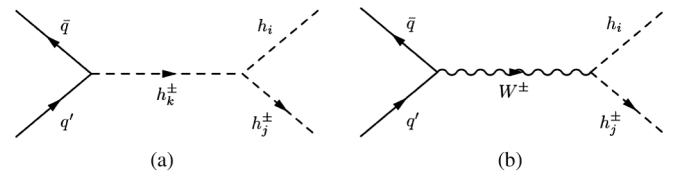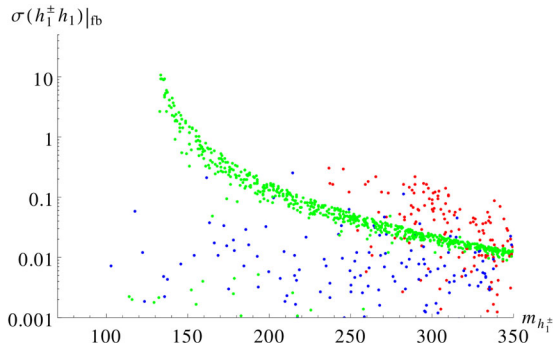

FIG. 23. The production cross section of the light charged Higgs boson $h_1^\pm$ associated with the a_1 boson versus the light charged Higgs boson mass $m_{h_1^\pm}$.

charged Higgs boson and another mediated by the $W^\pm$ boson. However, the charged Higgs-mediated diagrams are suppressed, for the same reasons discussed earlier regarding the associated Z production. Both the triplet and doublet Higgs bosons couple to the $SU(2)$ gauge boson $W^\pm$. However, a careful look at the vertex, given in Eq. (24), shows that their mixing angles can have relative signs. In general, their couplings associated with neutral Higgs bosons have to be doublet (triplet) type for doublet-(triplet-) type charged Higgs bosons.

This behavior can be seen in Fig. 21, where we plot the production cross section versus the mass of the lightest charged Higgs boson, $m_{h_1^\pm}$. The color code for the charged Higgs boson remains as before. It is quite evident that, for a tripletlike charged Higgs boson, the cross sections associated with h_1, which is mostly doublet, are very small, except for the $\lambda_T \simeq 0$ points. We can see the enhanced cross section for the mostly doublet charged Higgs boson associated with a doubletlike h_1 (red points). The situation is different for $\lambda_T \simeq 0$, where it is easy to produce a mostly triplet charged Higgs boson in this channel due to the enhancement of the $h_1^\pm - W^\mp - h_1$ coupling, given in Eq. (24). This is due to the fact that, for $\lambda_T \simeq 0$, the rotation angles $\mathcal{R}_{12}^C$ and $\mathcal{R}_{14}^C$ of the triplet sector, which appear in the coupling given in Eq. (24), take the same sign (in the decoupling limit, see Fig. 6).

D. Associated a_1

Similarly, we can also produce the charged Higgs boson associated with a pseudoscalar Higgs boson, as shown in

Fig. 22. Here, we also include the two contributions coming from $h_i^\pm$ and $W^\pm$, respectively, even though, as before, the contribution from the charged Higgs propagator is negligible. Figure 23 presents a variation of the cross section with the mass of the lightest charged Higgs boson. The cross section stays very low for the tripletlike points (the green ones) and reaches a maximum of around 10 fb for doublet- and mixedlike points (the red and blue ones). For $\lambda_T \simeq 0$ points, the triplet (T_1^+, T_2^{-*}) rotation angles $\mathcal{R}_{i2,i4}^C$ appear with a relative sign in the coupling $h_i^\pm - W^\mp - a_j$, as can be seen in Eq. (24). The $h_1^\pm a_1$ cross section thus gets a suppression in the decoupling limit, i.e., for $|\lambda_T| \simeq 0$, unlike the $h_i h_1^\pm$ case, as discussed in the previous section.

E. Charged Higgs pair production

Here, we move to the description of the charged Higgs pair production for the lightest charged Higgs boson $h_1^\pm$. The Feynman diagrams for this process are given in Fig. 24, with the neutral Higgses and Z, γ bosons contributing to the process. However, if the lightest charged Higgs boson $h_1^\pm$ is tripletlike, the diagrams of Fig. 24(a) make less of a contribution to the cross section. In fact, a_1 is selected to be singletlike, so it does not couple to the fermions, and the diagram with h_{125} in the propagator is subdominant. The reason is that the coupling $g_{h_1^\pm h_1^\mp h_1}$ of a totally doublet scalar Higgs boson with two totally triplet charged Higgs bosons is prevented by gauge invariance. The triplet charged Higgs pair production is more suppressed than the single tripletlike charged Higgs production via a
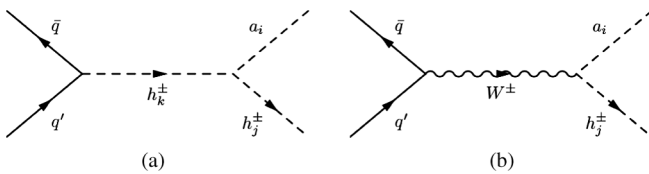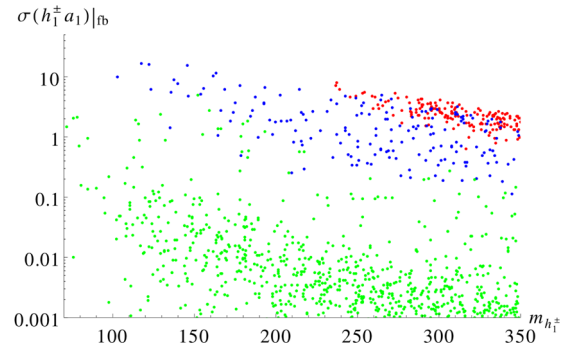

FIG. 22. Figures (a,b) describe the production of charged Higgs boson in association with a_i boson via $h_k^\pm$ and $W^\pm$ boson exchange.
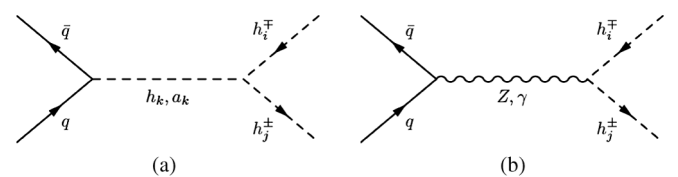

FIG. 24. Figures (a,b) describe the production of charged Higgs boson pair via h_k/a_k and Z/γ boson exchange.
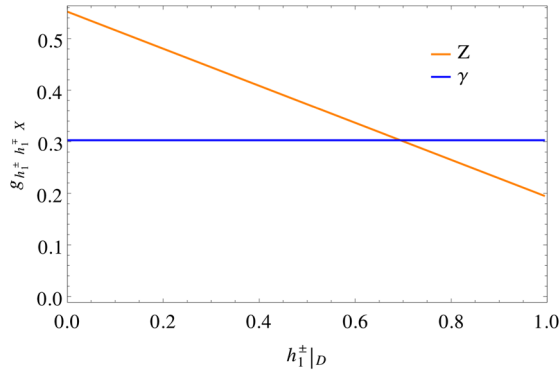
FIG. 25.   Value of the coupling $g_{h_1^\pm h_1^\mp X}$ as a function of the doublet fraction of the lightest charged Higgs boson. In the case of the photon, this coupling is simply the value of the electric charge.

FIG. 27.   The Feynman diagram for the charged Higgs production via vector boson fusion at the LHC.

doubletlike neutral Higgs boson. In that case, the pair production cross section via off-shell doublet-type neutral Higgs mediation (h_{125}) in the s-channel via gluon-gluon fusion is below $\mathcal{O}(10^{-6})$ fb. Hence, for a tripletlike $h_1^\pm$, the diagrams of Fig. 24(b) are the most relevant ones. The coupling of a pair of $h_1^\pm$'s to the Z and γ bosons is shown in Fig. 25 as a function of the doublet fraction. The coupling $g_{h_1^\pm h_1^\mp \gamma}$ is independent of the structure of $h_1^\pm$, as it should be because of the $U(1)_{em}$ symmetry. In fact, the value of this coupling is simply the value of the electric charge. Conversely, the coupling of the Z boson to a pair of charged Higgses depends on the structure of the charged Higgs. When the charged Higgs is totally doublet, its coupling approaches the MSSM value $\frac{g_L}{2}\frac{\cos 2\theta_w}{\cos \theta_w}$. If the charged Higgs is totally triplet, the value of the coupling is $g_L \cos \theta_w$, the same as the $W^\pm - W^\mp - Z$ interaction. In Fig. 26 we show the variation of the cross sections with respect to the lightest charged Higgs boson mass, $m_{h_1^\pm}$. The color code of the points is as in the previous figures. We can see that, for tripletlike points with a mass of ~100 GeV, the cross section reaches around a picobarn. This large cross section makes this production a viable channel to be probed at the LHC for the light triplet-type charged Higgs boson. We discuss the corresponding phenomenology in Sec. VIII.
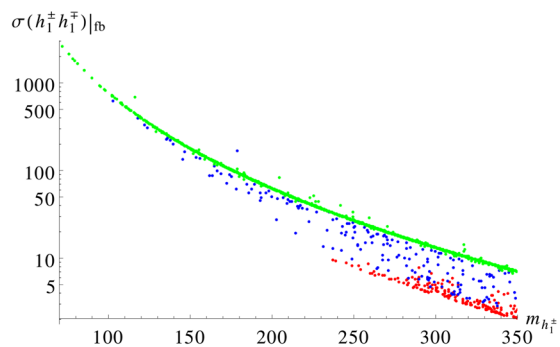
F. Vector boson fusion

Neutral Higgs boson production via vector boson fusion is the second most dominant production mode in the SM. Even in the 2HDM or the MSSM, this production mode of the neutral Higgs boson is one of the leading ones. However, no such channel exists for a charged Higgs boson, as the $h_i^\pm - W^\mp - Z$ vertex is zero at tree level, as long as custodial symmetry is preserved. The introduction of a $Y = 0$ triplet breaks the custodial symmetry at tree level, giving a nonzero $h_i^\pm - W^\mp - Z$ vertex, as shown in Eq. (27). This vertex gives rise to the striking production channel of the vector boson fusion into a single charged Higgs boson, which is absent in the MSSM and in the 2HDM at tree level. This is a signature of the triplets with $Y = 0, \pm 2$ which breaks custodial symmetry at tree level.

Figure 27 describe the charged Higgs production via vector boson fusion and Fig. 28 shows the cross-section variation with respect to the lightest charged Higgs boson mass, $m_{h_1^\pm}$. As expected, doubletlike points (in red) have very small cross sections, and for the mixed points (in blue) we see a little enhancement. Green points describe the cross sections for the tripletlike points. We see that a tripletlike charged Higgs boson does not necessarily guarantee large values for the cross section. As one can notice in Eq. (27), the coupling $g_{h_1^\pm W^\mp Z}$ is a function of $\mathcal{R}_{12}^C$ and $\mathcal{R}_{14}^C$, and their relative sign plays an important role. From Fig. 9 we see that only in the decoupling limit, where $\lambda_T = 0$, do both $\mathcal{R}_{12}^C$ and $\mathcal{R}_{14}^C$ take the

FIG. 26.   The production cross section of light charged Higgs boson pair $h_1^\pm h_1^\mp$ versus the light charged Higgs boson mass $m_{h_1^\pm}$.
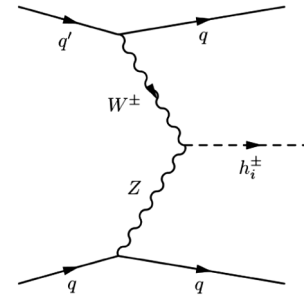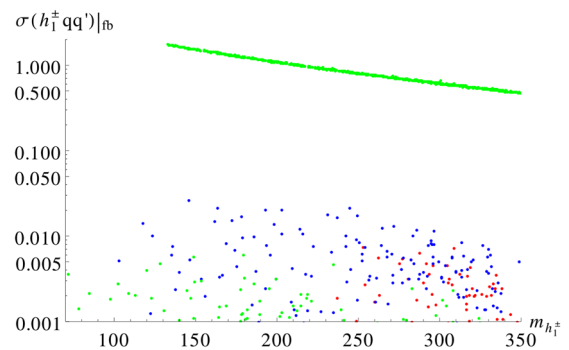

FIG. 28.   The production cross section of a light charged Higgs boson via vector boson fusion versus the light charged Higgs boson mass $m_{h_1^\pm}$.
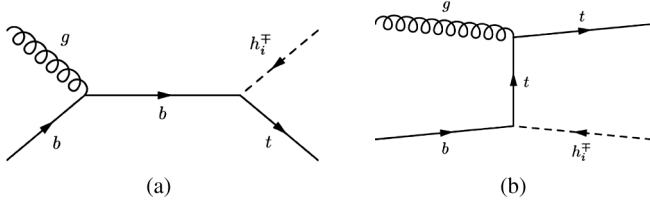
FIG. 29.   Figures (a,b) describe the production of charged Higgs boson in association with top quark via b and t exchange.

same sign, thereby enhancing the $h_1^\pm - W^\mp - Z$ coupling—and thus the cross section. It can been seen that only for lighter masses of ~ 150–200 GeV are the cross sections around a few femtobarns. Such tripletlike charged Higgs bosons can be probed at the LHC as a single charged Higgs production channel without the top quark. This channel can thus be used to distinguish among other known single charged Higgs production modes associated with the top quark, which characterizes a doubletlike charged Higgs boson.

G. Associated top quark

In the TNMSSM the triplet sector does not couple to fermions, which causes a natural suppression of the production of a tripletlike charged Higgs associated with a top quark. The only way for this channel to be allowed is via the mixing with doublets. Figure 29 shows the Feynman diagrams of such production processes, which are dominant and take place via a b quark and gluon fusion. They are highly dependent on the value of $\tan\beta$ [27,28]. Figure 30(b) shows the production cross section as a function of the lightest charged Higgs boson mass, where the green points correspond to linear combinations which are mostly triplet ($\gtrsim 90\%$), while red points correspond to those which are mostly doublet ($\gtrsim 90\%$) and the blue points are of mixed type. Tripletlike points have a naturally suppressed cross section, whereas the doubletlike points have a large cross section that can be $\sim$ a picobarn. The mixed points lie in between, with cross sections of $\mathcal{O}(100)$ fb. One can also notice a certain enhanced line in the green points which
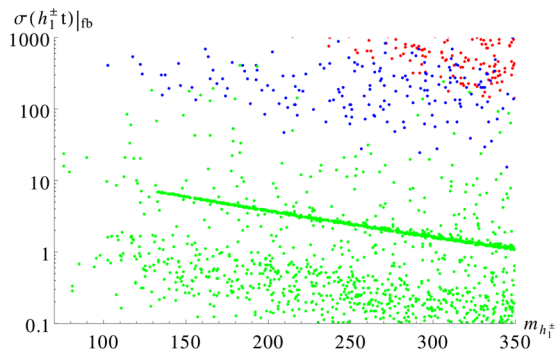

FIG. 30.   The production cross section of light charged Higgs boson associated with the top quark versus the light charged Higgs boson mass $m_{h_1^\pm}$.

correspond to $|\lambda_T| \simeq 0$. As explained in the previous sections, in this limit some portion $[\sim (\frac{v_T}{v})^2]$ of the lightest charged Higgs boson $h_1^\pm$ remains doublet type, as shown in Fig. 5, and is responsible for the enhancement of the cross section.

Thus, not finding a charged Higgs boson in this channel does not mean that it is completely ruled out, simply that it can come from a higher representation of $SU(2)$.

VIII. CHARGED HIGGS BOSON PHENOMENOLOGY

As was pointed out before, the TNMSSM with a Z_3 symmetry allows for a very light singletlike pseudoscalar in its spectrum, which turns into a pseudo-NG mode in the limit of small soft parameters A_i [13]. The existence of such a light and still hidden scalar prompts the decay of a light charged Higgs boson $h_1^\pm \rightarrow a_1 W^\pm$. Of course, the gauge invariant structure of the vertex further restricts such a decay mode, which is only allowed by the mass mixing of the singlet with the doublets or the triplet. In the extended supersymmetric scenarios with only a triplet, one cannot naturally obtain such a light tripletlike pseudoscalar because imposing Z_3 symmetry would be impossible due to the existence of a μ term, which is necessary to satisfy the lightest chargino mass bound [11]. The existence of a light pseudoscalar mode has been observed and studied in the context of the NMSSM [29–32]. Unlike the NMSSM, in the TNMSSM with a Z_3 symmetry, the decay $h_1^\pm \rightarrow ZW^\pm$ is possible for a triplet-type light charged Higgs boson. Below, we discuss the phenomenology of such charged Higgs bosons at the LHC.

For this phenomenological analysis, we have selected three benchmark points, BP1, BP2, and BP3, given in Table II. All of them are characterized by a tripletlike charged Higgs boson $h_1^\pm$, which makes the charged Higgs branching fractions into fermions, e.g., $\mathcal{B}(h_1^\pm \rightarrow \tau\nu_\tau)$ or $\mathcal{B}(h_1^\pm \rightarrow tb)$, strongly suppressed. We choose this scenario with a tripletlike charged Higgs boson to look for new physics signals that are not there in the 2HDM, the MSSM, or the NMSSM. The benchmark points maximize the following decay modes.

(i)   BP1: $\sigma_{pp \rightarrow h_1^\pm h_1^\mp} \times \mathcal{B}(h_1^\pm \rightarrow a_1 W^\pm) \mathcal{B}(h_1^\mp \rightarrow ZW^\mp)$.

(ii)   BP2: $\sigma_{pp \rightarrow h_1^\pm h_1^\mp} \times \mathcal{B}(h_1^\pm \rightarrow a_1 W^\pm) \mathcal{B}(h_1^\mp \rightarrow a_1 W^\pm)$.

(iii)   BP3: $\sigma_{pp \rightarrow h_1^\pm h_1^\mp} \times \mathcal{B}(h_1^\pm \rightarrow ZW^\mp) \mathcal{B}(h_1^\mp \rightarrow ZW^\mp)$.

We will discuss the final state searches along with dominant SM backgrounds below, starting with BP1 to BP3. A detailed collider study is in preparation [33].

If the lightest charged Higgs boson is pair produced, it can have the following decay topologies:

$$pp \rightarrow h_1^\pm h_1^\mp$$
$$\rightarrow a_1 W^\pm Z W^\mp$$
$$\rightarrow 2\tau(2b) + 2j + 3\ell + \not{E}_T$$
$$\rightarrow 2\tau(2b) + 4\ell + \not{E}_T. \tag{31}$$

TABLE II.　The mass of $h_1^\pm$, the mass of a_1, and the relevant branching ratios for the three benchmark points used in the phenomenological analysis.

	$m_{h_1^\pm}$	m_{a_1}	$\mathcal{B}(a_1 W^\pm)$	$\mathcal{B}(ZW^\pm)$	$\mathcal{B}(\tau\nu_\tau)$
BP1	179.69	41.22	9.7×10^{-1}	2.1×10^{-2}	1.3×10^{-4}
BP2	112.75	29.77	9.9×10^{-1}	6.3×10^{-5}	5.5×10^{-3}
BP3	172.55	48.94	6.3×10^{-5}	9.8×10^{-1}	2.4×10^{-3}

Equation (31) shows that when one of the charged Higgs bosons decays to $a_1 W^\pm$, which is a signature of the existence of a singlet-type pseudoscalar, the other one decays to $ZW^\pm$, which is the triplet signature. Thus, we end up with an $a_1 + 2W^\pm + Z$ intermediate state. Depending on the decays of the gauge bosons (hadronic or leptonic) and that of the light pseudoscalar (into b or τ pairs), we can have final states with a multilepton plus two b- or τ-jets. The trilepton and four-lepton backgrounds are generally rather low in the SM. In this case they are further tagged with a b- or τ-jet pair, which makes these channels cleaner. As mentioned earlier, the detailed signal and background study is in progress as a separate study in [33]. However, in Table III we look for $\geq 3\ell + 2\tau + \not{E}_T$ and $\geq 3\ell + 2b + \not{E}_T$ final state event numbers at an integrated luminosity of 1000 fb^{-1} for both the BP1 and dominant SM backgrounds. The demand $\geq 3\ell$ over 4ℓ was chosen to enhance the signal numbers. The kinematical cuts on the momentum and various isolation cuts and tagging efficiencies for b-jets [34] and τ-jets [35] reduce the final state numbers. The b-tagging efficiency has been chosen to be 0.5 and the τ-jet tagging efficiency varies a lot with the momentum of the τ-jet (30%–70%) are taken into account while giving the final state numbers. For $\geq 3\ell + 2\tau + \not{E}_T$ and $\geq 3\ell + 2b + \not{E}_T$ final states, the dominant backgrounds mainly come from triple gauge boson productions ZZZ and ZWZ, respectively. We can see that $\geq 3\ell + 2b + \not{E}_T$ reaches around 3σ of signal significance at an integrated luminosity of 1000 fb^{-1}. However, a point with larger branching to both the $aW^\pm$ and $ZW^\pm$ decay modes can be probed with much earlier data.

In the case of a TESSM [8,11], we have only the triplet signature of charged Higgs decaying into $ZW^\pm$, which

TABLE III.　The final state numbers for the benchmark points and backgrounds at an integrated luminosity of 1000 fb^{-1}.

	Decay channels		No. of events	
			Signal	Backgrounds
BP1	$a_1 W^\pm ZW^\mp$	$\geq 3\ell + 2\tau + \not{E}_T$	1	6
		$\geq 3\ell + 2b + \not{E}_T$	21	39
BP2	$a_1 W^\pm \tau\nu_\tau$	$3\tau + 1\ell + \not{E}_T$	13	< 1
	$a_1 W^\pm a_1 W^\mp$	$2b + 2\tau + 2\ell + \not{E}_T$	164	38
BP3	$ZW^\pm \tau\nu_\tau$	$1\tau + 3\ell + \not{E}_T$	9	19
		$\geq 5\ell + \not{E}_T$	228	23
	$ZW^\pm ZW^\mp$	$\geq 1\ell + 2b + 2\tau + \not{E}_T$	29	246

carries a different signature with respect to the doubletlike charged Higgs boson. On the other hand, in the NMSSM we only have $a_1 W^\pm$ decay [29–32], which is characterized by a different signature with respect to the MSSM [5,6]. In comparison, Eq. (31) provides a golden plated mode in the search for an extended Higgs sector, as predicted by the TNMSSM. Finding both the $a_1 W^\pm$ and $ZW^\pm$ decay modes at the LHC can prove the existence of both a singlet and a triplet of the model. However, as we can see in Fig. 31, it is very difficult to find points where both $\mathcal{B}(h_1^\pm \to ZW^\pm)$ and $\mathcal{B}(h_1^\pm \to a_1 W^\pm)$ are enhanced at the same time. Nevertheless, as the final states carry the signatures of both singlet- and triplet-type Higgs bosons, it is worth exploring for a high luminosity at the LHC—or at an even higher energy (more than 14 TeV) at the LHC in the future.

The light charged Higgs boson can also decay to $\tau\nu$ for $m_{h_1^\pm} < m_t$ and to tb for $m_{h_1^\pm} > m_t$ via its doublet fraction. The charged Higgs pair production then has the signatures given in Eqs. (32) and (33), with one of the charged Higgs bosons decaying to $\tau\nu$ and the other to $a_1 W^\pm$ or $ZW^\pm$, respectively. Equations (32) and (33) probe the existence of singlet, doublet, and triplet representations at the same time. The final states with one or more τ-jets along with a charged lepton reduce the SM backgrounds, but $t\bar{t}Z$ and $tZW^\pm$ nevertheless contribute:
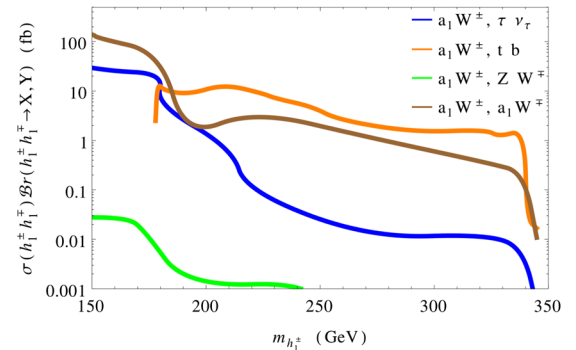
(a)
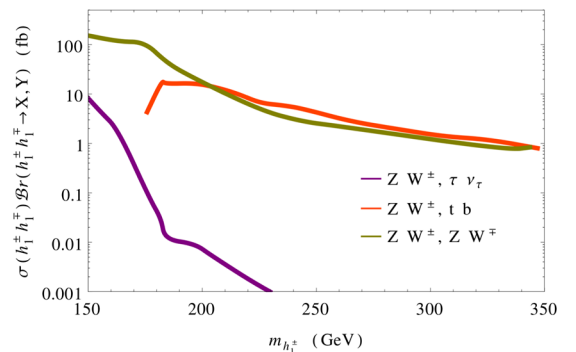
(b)

FIG. 31.　The signal strength for the pair production of the lightest charged Higgs boson in the intermediate channels of (a) Eqs. (31), (32), (34), (36), and (b) (33), (35), and (37) as a function of the mass of the lightest charged Higgs boson.

$$pp \to h_1^{\pm} h_1^{\mp}$$
$$\to a_1 W^{\pm} \tau \nu$$
$$\to 3\tau/(2b + 1\tau) + 1\ell + \not{E}_T, \qquad (32)$$

$$pp \to h_1^{\pm} h_1^{\mp}$$
$$\to ZW^{\pm} \tau \nu$$
$$\to 1(3)\tau + 3(1)\ell + \not{E}_T. \qquad (33)$$

Thus, these final states would play a very crucial role in determining whether the mechanism of EWSB incorporates a finer structure with respect to our current description, with a single Higgs doublet. In Table III we present the number of events in the $3\tau + 1\ell + \not{E}_T$ final state for the channel $a_1 W^{\pm} \tau \nu_{\tau}$, and in the $1\tau + 3\ell + \not{E}_T$ final state for the channel $ZW^{\pm} \tau \nu_{\tau}$ at an integrated luminosity of 1000 fb^{-1}. As already stated, we chose a tripletlike charged Higgs boson $h_1^{\pm}$, and hence the branching in $\tau \nu_{\tau}$ is suppressed, being a signature decay mode for a doublet-type charged Higgs boson. In both cases the dominant backgrounds are the triple gauge bosons ZZZ and ZWZ. We can see that $3\ell + 1\tau + \not{E}_T$ reaches more than 3σ of the signal significance at an integrated luminosity of 1000 fb^{-1}. There are, of course, two other possibilities for the decays of a pair of charged Higgs bosons—that is, when both of the charged Higgs bosons decay to $a_1 W^{\pm}$ or $ZW^{\pm}$:

$$pp \to h_1^{\pm} h_1^{\mp}$$
$$\to a_1 W^{\pm} a_1 W^{\mp}$$
$$\to 2\tau + 2b + 2j + 1\ell + \not{E}_T$$
$$\to 4\tau(4b) + 2\ell + \not{E}_T$$
$$\to 2b + 2\tau + 2\ell + \not{E}_T, \qquad (34)$$

$$pp \to h_1^{\pm} h_1^{\mp}$$
$$\to ZW^{\pm} ZW^{\mp}$$
$$\to 2j + 4\ell + \not{E}_T$$
$$\to 6\ell + \not{E}_T$$
$$\to 2b + 2\tau + 2\ell + \not{E}_T. \qquad (35)$$

These channels can prove the existence of singlet and triplet representations separately. For the decay channel $h_1^{\pm} h_1^{\mp} \to a_1 W^{\pm} a_1 W^{\mp}$, we have considered the $2b + 2\tau + 2\ell + \not{E}_T$ final state for the signal and background analysis. This is because the final states with $\geq 1\ell$ have $\bar{t}t$ as the dominant background, and hence they are strongly suppressed. For $2b + 2\tau + 2\ell + \not{E}_T$ the dominant backgrounds are ZZZ and $\bar{t}tZ$, and we can see from Table III that the signal significance is more than 10σ for an integrated luminosity of 1000 fb^{-1}. A signal significance of 5σ can be achieved with an integrated luminosity of ≈ 200 fb^{-1} at the LHC, with a 14 TeV center of mass energy.

In the case of $h_1^{\pm} h_1^{\mp} \to ZW^{\pm} ZW^{\mp}$, we look into the $\geq 5\ell + \not{E}_T$ and $\geq 1\ell + 2b + 2\tau + \not{E}_T$ final states, where the demand $\geq 1\ell$ over 2ℓ was chosen to enhance the signal numbers. The $\geq 5\ell + \not{E}_T$ has the triple gauge bosons ZZZ and ZWZ as the dominant backgrounds. This is one of the cleanest final states, and we can see from Table III that it has a signal significance of more than 14σ at an integrated luminosity of 1000 fb^{-1}. The integrated luminosity for a signal significance of 5σ is 120 fb^{-1}. The dominant backgrounds for the $\geq 1\ell + 2b + 2\tau + \not{E}_T$ final state are the triple gauge bosons ZZZ and ZWZ, as well as $\bar{t}tZ$. The $\bar{t}tZ$ background is the most dominant one in this case and suppresses the signal significance, as one can immediately realize by looking at Table III.

For charged Higgs bosons heavier than the top quark, the channel $h_1^{\pm} \to tb$ is kinematically allowed. If one of the charged Higgs decays to tb and the other one decays to $a_1 W^{\pm}$, we have the final states given by Eq. (36). When the other charged Higgs boson decays to $ZW^{\pm}$, the production of $h_1^{\pm} h_1^{\mp}$ results in the final states of Eq. (37),

$$pp \to h_1^{\pm} h_1^{\mp}$$
$$\to a_1 W^{\pm} tb$$
$$\to 2\tau + 2b + 2W$$
$$\to 2\tau + 2b + 2\ell + \not{E}_T, \qquad (36)$$

$$pp \to h_1^{\pm} h_1^{\mp}$$
$$\to ZW^{\pm} tb$$
$$\to 2\tau + 2b + 2W$$
$$\to 2\tau + 2b + 2\ell + \not{E}_T$$
$$\text{or} \qquad 2b + 4\ell + \not{E}_T. \qquad (37)$$

The signal related to the intermediate states of the pair production and the decays of the lightest charged Higgs boson in the channels of Eqs. (31), (32), (33), (36), and (37) is reported in Fig. 31. We can clearly see that, for a light charged Higgs boson ($m_{h_1^{\pm}} \gtrsim 200$ GeV), the decay modes in a light pseudoscalar can be probed rather easily at the LHC, but probing $a_1 W^{\pm}$ and $ZW^{\mp}$—i.e., the existence of a light pseudoscalar and the triplet decay modes together—requires a higher luminosity.

Another signature of this model could be the existence of the heavier charged Higgs bosons $h_{2,3}^{\pm}$, which could be produced at the LHC. For our selection points, $h_2^{\pm}$ is tripletlike and $h_3^{\pm}$ is doubletlike. Following our discussion in Sec. VI, such heavy charged Higgs can decay dominantly to $a_1 h_1^{\pm}$ or $h_1 h_1^{\pm}$, as shown in Eqs. (38) and (39). The lighter charged Higgs can then decay into final states with $a_1 W^{\pm}$ or $ZW^{\pm}$, giving the $2\tau(2b) + 3\ell + \not{E}_T$ and $4\tau(4b) + 1\ell + \not{E}_T$ final states,

$$pp \to h_{2,3}^{\pm} + X \to a_1/h_1 h_1^{\mp}$$
$$\to 2\tau(2b) + ZW^{\pm}$$
$$\to 2\tau(2b) + 3\ell + \not{E}_T, \qquad (38)$$

$$pp \to h_{2,3}^{\pm} + X \to a_1/h_1 h_1^{\mp}$$
$$\to 2\tau(2b) + a_1 + W^{\pm}$$
$$\to 4\tau(4b) + 1\ell + \not{E}_T. \qquad (39)$$

Searching for the above signatures is certainly necessary—not only in order to discover a charged Higgs boson but also to determine whether scalars in higher representations of $SU(2)$ are involved in the mechanism of EWSB.

IX. DISCUSSION

In this article we present a detailed analysis of the charged Higgs sector of the TNMSSM, considering both doublet- and tripletlike cases, as predicted by the triplet-singlet extension of the MSSM. We focus our attention on a typical mass spectrum with a doubletlike CP-even Higgs boson of around 125 GeV, a light tripletlike charged Higgs boson, and a light singletlike pseudoscalar. The existence of a light singletlike pseudoscalar and a tripletlike charged Higgs boson enrich the phenomenology at the LHC and at future colliders.

In general, we expect to have a mixing between doublet- and triplet-type charged Higgs. We find that in the decoupling limit, $\lambda_T \simeq 0$, one should expect two tripletlike and one doubletlike massive charged Higgs bosons. However, since the Goldstone boson is a linear combination which includes a triplet contribution $\sim v_T/v$ [see Eq. (23)], one of the massive eigenstates triplets cannot be 100% tripletlike.

Recent searches by both CMS [5] and ATLAS [6] are conducted for a charged Higgs of mainly the doublet type and coupled to fermions. For this reason, such a state can be produced in association with the top quark and can decay to $\tau\nu$. Clearly, these searches have to be reinvestigated in order to probe the possibility of triplet representations of $SU(2)$ in the Higgs sector.

The breaking of the custodial symmetry via a nonzero triplet VEV generates a $h_i^{\pm} - W^{\mp} - Z$ vertex at tree level in the TNMSSM. This leads to the vector boson fusion channel for the charged Higgs boson, which is not present in the MSSM or the 2HDM. On top of that, the Z_3 symmetric superpotential of the TNMSSM has a light pseudoscalar a_1 as a pseudo-NG mode of a global $U(1)$ symmetry, known as the R axion in the literature. However, the latter can also be found in the context of the Z_3 symmetric NMSSM. In this case, the light charged Higgs boson can decay to $a_1 W^{\pm}$ [29–32], just like in the TNMSSM. In the context of a CP-violating MSSM, such modes can arise due to the possibility of a light Higgs boson h_1 and of CP-violating interactions. A charged Higgs boson can decay to $h_1 W^{\pm}$ [36], just as in our case. Therefore, one of the challenges at

the LHC will be to distinguish among such models once such a mode is discovered.

Triplet charged Higgs bosons with $Y = 0$, however, have some distinctive features because they do not couple to the fermions, while the fusion channel $ZW^{\pm}$ is allowed. The phenomenology of such a tripletlike charged Higgs boson has already been studied in the context of the TESSM [11]. Such charged Higgs bosons also affect the predictions of B observables [8,9] for missing the coupling to fermions and to the Z boson. However, in the TESSM, even though the charged Higgs boson decays to $ZW^{\pm}$ [11], the possibility of a light pseudoscalar is not so natural [8–11]. Indeed, one way to distinguish between the TESSM and the TNMSSM is to exploit the prediction of a light pseudoscalar in the second model alongside the light triplet type charged Higgs boson.

We expect that such a Higgs in the TNMSSM will be allowed to decay both to $ZW^{\pm}$ and to $a_1 W^{\pm}$, the former being a feature of the triplet nature of this state and the latter of the presence of an R axion in the spectrum of the model. We are currently performing a detailed simulation of both the TESSM and the NMSSM in order to identify specific signatures which can be compared with the TNMSSM [33]. A complete simulation of the Standard Model background is also under way.

X. CONCLUSIONS

Tripletlike charged Higgs bosons do not couple to fermions [see Eq. (4)], which makes them hard to produce at the LHC. The nonzero triplet VEV breaks the custodial symmetry, and the consequences can be seen in nonzero $h_i^{\pm} - W^{\mp} - Z$ coupling. Thus, measurement of such a coupling or decay of the charged Higgs boson in $ZW^{\pm}$ can shed light on determining the role of the triplet in electroweak symmetry breaking. For this reason, we propose a few channels which can be probed at the LHC. Specifically, if the tripletlike charged Higgs bosons are pair produced at the LHC, it would be interesting to see if both the $a_1 W^{\pm}$ and $ZW^{\pm}$ decay modes can be probed. Finding these decay modes can surely serve as proof for the existence of both the singlet and the triplet in the mass spectrum. This can be a smoking gun signature for the TNMSSM at the LHC. The general fermiofobic nature, however, pushes this settlement to a higher luminosity at the LHC.

APPENDIX: MASS MATRIX OF THE HIGGS SECTOR

The symmetric mass matrices of the Higgs sector are given by

$$\mathcal{M}^S = \begin{pmatrix} m_{11}^S & m_{12}^S & m_{13}^S & m_{14}^S \\ & m_{22}^S & m_{23}^S & m_{24}^S \\ & & m_{33}^S & m_{34}^S \\ & & & m_{44}^S \end{pmatrix}, \qquad (A1)$$

$$\mathcal{M}^P = \begin{pmatrix} m_{11}^P & m_{12}^P & m_{13}^P & m_{14}^P \\ & m_{22}^P & m_{23}^P & m_{24}^P \\ & & m_{33}^P & m_{34}^P \\ & & & m_{44}^P \end{pmatrix}, \quad \text{(A2)}$$

$$\mathcal{M}^C = \begin{pmatrix} m_{11}^C & m_{12}^C & m_{13}^C & m_{14}^C \\ & m_{22}^C & m_{23}^C & m_{24}^C \\ & & m_{33}^C & m_{34}^C \\ & & & m_{44}^C \end{pmatrix}, \quad \text{(A3)}$$

where we have used the following abbreviations:

$$m_{11}^S = \frac{1}{4v_u}(2v_d(\sqrt{2}A_S v_S - v_T(A_T + \sqrt{2}v_S\lambda_T\lambda_{TS}) + \lambda_S(\kappa v_S^2 + v_T^2\lambda_{TS})) + v_u^3(g_L^2 + g_Y^2))$$

$$m_{12}^S = \frac{1}{2}(-\sqrt{2}A_S v_S + v_T(A_T + \sqrt{2}v_S\lambda_T\lambda_{TS}) - \lambda_S(\kappa v_S^2 + v_T^2\lambda_{TS})) - \frac{1}{4}v_d v_u(g_L^2 + g_Y^2 - 2(2\lambda_S^2 + \lambda_T^2))$$

$$m_{13}^S = -\frac{A_S v_T}{\sqrt{2}} + v_d\left(\frac{\lambda_T v_T\lambda_{TS}}{\sqrt{2}} - \kappa\lambda_S v_S\right) + \frac{1}{2}v_u\lambda_S(2\lambda_S v_S - \sqrt{2}\lambda_T v_T)$$

$$m_{14}^S = \frac{1}{2}(v_d(A_T - 2\lambda_S v_T\lambda_{TS}) + \sqrt{2}v_S\lambda_T(v_d\lambda_{TS} - v_u\lambda_S) + v_u\lambda_T^2 v_T)$$

$$m_{22}^S = \frac{1}{4v_d}(2v_u(\sqrt{2}A_S v_S - v_T(A_T + \sqrt{2}v_S\lambda_T\lambda_{TS}) + \lambda_S(\kappa v_S^2 + v_T^2\lambda_{TS})) + v_d^3(g_L^2 + g_Y^2))$$

$$m_{23}^S = -\frac{A_S v_u}{\sqrt{2}} + \frac{1}{2}v_d\lambda_S(2\lambda_S v_S - \sqrt{2}\lambda_T v_T) + v_u\left(\frac{\lambda_T v_T\lambda_{TS}}{\sqrt{2}} - \kappa\lambda_S v_S\right)$$

$$m_{24}^S = \frac{1}{2}(v_u(A_T - 2\lambda_S v_T\lambda_{TS}) + \sqrt{2}v_S\lambda_T(v_u\lambda_{TS} - v_d\lambda_S) + v_d\lambda_T^2 v_T)$$

$$m_{33}^S = \frac{1}{4v_S}(\sqrt{2}v_T(\lambda_T(\lambda_S(v_d^2 + v_u^2) - 2v_d v_u\lambda_{TS}) - 2A_{TS}v_T) + 2\sqrt{2}A_S v_d v_u + 2\sqrt{2}A_\kappa v_S^2 + 8\kappa^2 v_S^3)$$

$$m_{34}^S = \frac{1}{4}(4\sqrt{2}A_{TS}v_T - \sqrt{2}\lambda_S\lambda_T(v_d^2 + v_u^2) + 2\lambda_{TS}(\sqrt{2}v_d v_u\lambda_T + 4v_S v_T(\kappa + 2\lambda_{TS})))$$

$$m_{44}^S = \frac{1}{4v_T}(-2v_d v_u(A_T + \sqrt{2}v_S\lambda_T\lambda_{TS}) + \sqrt{2}v_d^2\lambda_S v_S\lambda_T + \sqrt{2}v_u^2\lambda_S v_S\lambda_T + 8v_T^3\lambda_{TS}^2)$$

$$m_{11}^P = \frac{v_d}{2v_u}((\sqrt{2}A_S v_S - v_T(A_T + \sqrt{2}v_S\lambda_T\lambda_{TS}) + \lambda_S(\kappa v_S^2 + v_T^2\lambda_{TS})))$$

$$m_{12}^P = \frac{1}{2}(\sqrt{2}A_S v_S - v_T(A_T + \sqrt{2}v_S\lambda_T\lambda_{TS}) + \lambda_S(\kappa v_S^2 + v_T^2\lambda_{TS}))$$

$$m_{13}^P = \frac{1}{2}v_d(\sqrt{2}A_S - 2\kappa\lambda_S v_S + \sqrt{2}\lambda_T v_T\lambda_{TS})$$

$$m_{14}^P = -\frac{1}{2}v_d(A_T + \lambda_{TS}(2\lambda_S v_T - \sqrt{2}v_S\lambda_T))$$

$$m_{22}^P = \frac{v_u}{2v_d}((\sqrt{2}A_S v_S - v_T(A_T + \sqrt{2}v_S\lambda_T\lambda_{TS}) + \lambda_S(\kappa v_S^2 + v_T^2\lambda_{TS})))$$

$$m_{23}^P = \frac{1}{2}v_u(\sqrt{2}A_S - 2\kappa\lambda_S v_S + \sqrt{2}\lambda_T v_T\lambda_{TS})$$

$$m_{24}^P = -\frac{1}{2}v_u(A_T + \lambda_{TS}(2\lambda_S v_T - \sqrt{2}v_S\lambda_T))$$

$$m_{33}^P = \frac{v_T}{4v_S}((\sqrt{2}\lambda_T(\lambda_S(v_d^2 + v_u^2) - 2v_d v_u\lambda_{TS})$$
$$- 2v_T(\sqrt{2}A_{TS} + 4\kappa v_S\lambda_{TS})) + 2\sqrt{2}A_S v_d v_u - 6\sqrt{2}A_\kappa v_S^2 + 8\kappa v_d v_u\lambda_S v_S)$$

$$m_{34}^P = \frac{1}{4}(-4\sqrt{2}A_{TS}v_T - \sqrt{2}\lambda_T(\lambda_S(v_d^2 + v_u^2) + 2v_d v_u \lambda_{TS}) + 8\kappa v_S v_T \lambda_{TS})$$

$$m_{44}^P = \frac{-2v_d v_u}{4v_T}((A_T + \lambda_{TS}(\sqrt{2}v_S\lambda_T - 4\lambda_S v_T)) + v_S(\sqrt{2}v_d^2\lambda_S\lambda_T - 8v_T(\sqrt{2}A_{TS} + \kappa v_S\lambda_{TS})) + \sqrt{2}v_u^2\lambda_S v_S\lambda_T)$$

$$m_{11}^C = \frac{1}{4}(2(\sqrt{2}v_S(A_S\cot\beta + \lambda_T v_T(2\lambda_S - \cot\beta\lambda_{TS})) + \cot\beta v_T(\lambda_S v_T\lambda_{TS} - A_T) + \kappa\cot\beta\lambda_S v_S^2) + \cos^2\beta v^2(g_L^2 - 2\lambda_S^2 + \lambda_T^2))$$

$$m_{12}^C = \frac{1}{4}v(\lambda_T(2v_S(\sin\beta\lambda_S - 2\cos\beta\lambda_{TS}) + \sqrt{2}\sin\beta\lambda_T v_T) - \sqrt{2}\sin\beta g_L^2 v_T)$$

$$m_{13}^C = \frac{1}{4}(2(v_T(A_T + \lambda_{TS}(\lambda_S v_T + \sqrt{2}v_S\lambda_T)) + \sqrt{2}A_S v_S + \kappa\lambda_S v_S^2) + \sin\beta\cos\beta v^2(g_L^2 - 2\lambda_S^2 + \lambda_T^2))$$

$$m_{14}^C = \frac{v}{4}(\sin\beta(\sqrt{2}v_T(g_L^2 - \lambda_T^2) + 2\lambda_S v_S\lambda_T) - 2\sqrt{2}A_T\cos\beta)$$

$$m_{22}^C = \frac{1}{4v_T}(v_T(v^2(\cos(2\beta)(g_L^2 - \lambda_T^2) + 2\sin(2\beta)\lambda_S\lambda_{TS}) - 4v_S(\sqrt{2}A_{TS} + \kappa v_S\lambda_{TS})) - A_T\sin(2\beta)v^2$$
$$+ 2v_T^3(g_L^2 - 2\lambda_{TS}^2) + \sqrt{2}v^2 v_S\lambda_T(\lambda_S - \sin(2\beta)\lambda_{TS}))$$

$$m_{23}^C = \frac{v}{4}(2\sqrt{2}A_T\sin\beta + \cos\beta(\sqrt{2}v_T(\lambda_T^2 - g_L^2) - 2\lambda_S v_S\lambda_T))$$

$$m_{24}^C = \sqrt{2}A_{TS}v_S - \frac{1}{2}g_L^2 v_T^2 + \lambda_{TS}(\kappa v_S^2 + v_T^2\lambda_{TS} - \sin\beta\cos\beta v^2\lambda_S)$$

$$m_{33}^C = \frac{1}{4}(2(\sqrt{2}v_S(A_S\tan\beta + \lambda_t v_T(2\lambda_S - \tan\beta\lambda_{TS})) + \tan\beta v_T(\lambda_S v_T\lambda_{TS} - A_T) + \kappa\tan\beta\lambda_S v_S^2)$$
$$+ \sin^2\beta g_L^2 v^2 + \sin^2\beta v^2(\lambda_T^2 - 2\lambda_S^2))$$

$$m_{34}^C = \frac{v}{4}(\cos\beta(\sqrt{2}v_T(g_L^2 - \lambda_T^2) - 2\lambda_S v_S\lambda_T) + 4\sin\beta v_S\lambda_T\lambda_{TS})$$

$$m_{44}^C = \frac{1}{4v_T}(v_T(v^2(\cos(2\beta)(\lambda_T^2 - g_L^2) + 2\sin(2\beta)\lambda_S\lambda_{TS}) - 4v_S(\sqrt{2}A_{TS} + \kappa v_S\lambda_{TS})) - A_T\sin(2\beta)v^2$$
$$+ 2v_T^3(g_L^2 - 2\lambda_{TS}^2) + \sqrt{2}v^2 v_S\lambda_T(\lambda_S - \sin(2\beta)\lambda_{TS}))$$

As explained already, the massive eigenvectors of the charged mass matrix are functions of all of the parameters of the model, including the parameters that are related to the singlet, e.g., v_S, λ_S, κ, whereas the Goldstone eigenvector is a function of the doublets and the triplet VEV only. This is also true for the eigenvectors of the pseudoscalar mass matrix. In this case, the Goldstone eigenvector is a function of the doublet VEV only.

[1] G. Aad *et al.* (ATLAS and CMS Collaborations), Combined Measurement of the Higgs Boson Mass in pp Collisions at $\sqrt{s} = 7$ and 8 TeV with the ATLAS and CMS Experiments, Phys. Rev. Lett. **114**, 191803 (2015); S. Chatrchyan *et al.* (CMS Collaboration), Measurement of Higgs boson production and properties in the WW decay channel with leptonic final states, J. High Energy Phys. 01 (2014) 096; Measurement of the properties of a Higgs boson in the four-lepton final state, Phys. Rev. D **89**, 092007 (2014).

[2] V. Khachatryan *et al.* (CMS Collaboration), Precise determination of the mass of the Higgs boson and tests of compatibility of its couplings with the standard model predictions using proton collisions at 7 and 8 TeV, Eur.

Phys. J. C **75**, 212 (2015); CMS Collaboration, Report No. CMS-PAS-HIG-13-002, 2013.

[3] ATLAS Collaboration, Report No. ATLAS-CONF-2015-007, 2015; G. Aad *et al.* (ATLAS Collaboration), Measurements of Higgs boson production and couplings in the four-lepton channel in pp collisions at center-of-mass energies of 7 and 8 TeV with the ATLAS detector, Phys. Rev. D **91**, 012006 (2015); Measurements of the Higgs boson production and decay rates and coupling strengths using pp collision data at $\sqrt{s} = 7$ and 8 TeV in the ATLAS experiment, Eur. Phys. J. C **76**, 6 (2016); Measurement of the Higgs boson mass from the $H \to \gamma\gamma$ and $H \to ZZ^* \to 4\ell$ channels with the ATLAS detector using

25 fb^{-1} of pp collision data, Phys. Rev. D **90**, 052004 (2014).

[4] R. Barbier, C. Berat, M. Besancon, M. Chemtob, A. Deandrea, E. Dudas, P. Fayet, S. Lavignac *et al.*, R-parity violating supersymmetry, Phys. Rep. **420**, 1 (2005).

[5] CMS Collaboration, Report No. CMS-PAS-HIG-14-020, 2014; V. Khachatryan *et al.* (CMS Collaboration), Search for a charged Higgs boson in pp collisions at $\sqrt{s} = 8$ TeV, J. High Energy Phys. 11 (2015) 018.

[6] G. Aad *et al.* (ATLAS Collaboration), Search for charged Higgs bosons decaying via $H^{\pm} \to \tau^{\pm}\nu$ in fully hadronic final states using pp collision data at $\sqrt{s} = 8$ TeV with the ATLAS detector, J. High Energy Phys. 03 (2015) 088.

[7] U. Ellwanger, C. Hugonie, and A. M. Teixeira, The next-to-minimal supersymmetric standard model, Phys. Rep. **496**, 1 (2010).

[8] P. Bandyopadhyay, K. Huitu, and A. Sabanci, Status of $Y = 0$ triplet Higgs with supersymmetry in the light of ~125 GeV Higgs discovery, J. High Energy Phys. 10 (2013) 091.

[9] P. Bandyopadhyay, S. Di Chiara, K. Huitu, and A. S. Keceli, Naturality vs perturbativity, B_s physics, and LHC data in triplet extension of MSSM, J. High Energy Phys. 11 (2014) 062.

[10] S. Di Chiara and K. Hsieh, Triplet extended supersymmetric standard model, Phys. Rev. D **78**, 055016 (2008).

[11] P. Bandyopadhyay, K. Huitu, and A. S. Keceli, Multi-lepton signatures of the triplet like charged Higgs at the LHC, J. High Energy Phys. 05 (2015) 026.

[12] J. R. Espinosa and M. Quiros, Higgs boson bounds in non-minimal supersymmetric standard models, Phys. Lett. **B279**, 92 (1992); Higgs triplets in the supersymmetric standard model, Nucl. Phys. **B384**, 113 (1992).

[13] P. Bandyopadhyay, C. Corianò, and A. Costantini, Perspectives on a supersymmetric extension of the standard model with a $Y = 0$ Higgs triplet and a singlet at the LHC, J. High Energy Phys. 09 (2015) 045.

[14] P. Bandyopadhyay, C. Corianò, and A. Costantini, Probing the hidden Higgs bosons of the $Y = 0$ triplet- and singlet-extended supersymmetric standard model at the LHC, J. High Energy Phys. 12 (2015) 127.

[15] T. Basak and S. Mohanty, Triplet-singlet extension of the MSSM with a 125 GeV Higgs and dark matter, Phys. Rev. D **86**, 075031 (2012); 130 GeV gamma ray line and enhanced Higgs di-photon rate from triplet-singlet extended MSSM, J. High Energy Phys. 08 (2013) 020; L. Basso, O. Fischer, and J. J. van der Bij, A singlet-triplet extension for the Higgs search at LEP and LHC, Europhys. Lett. **101**, 51004 (2013); O. Fischer and J. J. van der Bij, The scalar singlet-triplet dark matter model, J. Cosmol. Astropart. Phys. 01 (2014) 032.

[16] K. Agashe, A. Azatov, A. Katz, and D. Kim, Improving the tunings of the MSSM by adding triplets and singlet, Phys. Rev. D **84**, 115024 (2011).

[17] R. Barate *et al.* (LEP Working Group for Higgs Boson Searches and ALEPH, DELPHI, L3, and OPAL Collaborations), Search for the standard model Higgs boson at LEP, Phys. Lett. B **565**, 61 (2003); S. Schael *et al.* (LEP Working Group for Higgs Boson Searches and ALEPH, DELPHI, L3, and OPAL Collaborations), Search for

neutral MSSM Higgs bosons at LEP, Eur. Phys. J. C **47**, 547 (2006).

[18] J. Beringer *et al.* (Particle Data Group), Review of Particle Physics, Phys. Rev. D **86**, 010001 (2012).

[19] P. Franzini, D. Son, P. M. Tuts, S. Youssef, T. Zhao, J. Lee-Franzini, J. Horstkotte, C. Klopfenstein *et al.*, Limits on Higgs bosons, scalar quarkonia, and $\eta(B)$'s from radiative Υ decays, Phys. Rev. D **35**, 2883 (1987).

[20] J. S. Lee and S. Scopel, Lightest Higgs boson and relic neutralino in the MSSM with CP violation, Phys. Rev. D **75**, 075001 (2007).

[21] V. Khachatryan *et al.* (CMS and LHCb Collaborations), Observation of the rare $B_s^0 \to \mu^+\mu^-$ decay from the combined analysis of CMS and LHCb data, Nature (London) **522**, 68 (2015).

[22] E. Asakawa and S. Kanemura, The $H^{\pm}W^{\mp}Z^0$ vertex and single charged Higgs boson production via WZ fusion at the Large Hadron Collider, Phys. Lett. B **626**, 111 (2005).

[23] A. Djouadi, The anatomy of electro-weak symmetry breaking. II. The Higgs bosons in the minimal supersymmetric model, Phys. Rep. **459**, 1 (2008).

[24] F. Staub, SARAH3.2: Dirac gauginos, UFO output, and more, Comput. Phys. Commun. **184**, 1792 (2013).

[25] A. Pukhov, CalcHEP3.2: MSSM, structure functions, event generation, batchs, and generation of matrix elements for other packages, arXiv:hep-ph/0412191.

[26] J. Pumplin, D. R. Stump, J. Huston, H. L. Lai, P. Nadolsky, and W. K. Tung, New analysis, J. High Energy Phys. 07 (2002) 012; see also http://www.physics.smu.edu/scalise/cteq/.

[27] F. Borzumati and A. Djouadi, Lower bounds on charged Higgs bosons from LEP and Tevatron, Phys. Lett. B **549**, 170 (2002).

[28] D. J. Miller, S. Moretti, D. P. Roy, and W. J. Stirling, Detecting heavy charged Higgs bosons at the CERN LHC with four b-quark tags, Phys. Rev. D **61**, 055011 (2000).

[29] N. D. Christensen, T. Han, Z. Liu, and S. Su, Low-mass Higgs bosons in the NMSSM and their LHC implications, J. High Energy Phys. 08 (2013) 019.

[30] B. Coleppa, F. Kling, and S. Su, Charged Higgs search via $AW^{\pm}/HW^{\pm}$ channel, J. High Energy Phys. 12 (2014) 148.

[31] M. Drees, M. Guchait, and D. P. Roy, Signature of charged to neutral Higgs boson decay at the LHC in SUSY models, Phys. Lett. B **471**, 39 (1999).

[32] P. Bandyopadhyay, K. Huitu, and S. Niyogi, Non-standard charged Higgs decay at the LHC in next-to-minimal supersymmetric standard model, J. High Energy Phys. 07 (2016) 015.

[33] P. Bandyopadhyay, C. Corianò, and A. Costantini (to be published).

[34] I. R. Tomalin for the CMS Collaboration, b tagging in CMS, J. Phys. Conf. Ser. **110**, 092033 (2008).

[35] G. Bagliesi, Tau tagging at Atlas and CMS, arXiv:0707.0928; G. L. Bayatian *et al.* (CMS Collaboration), CMS physics technical design report, volume II: Physics performance, J. Phys. G **34**, 995 (2007).

[36] P. Bandyopadhyay and K. Huitu, Production of two Higgses at the Large Hadron Collider in CP-violating MSSM, J. High Energy Phys. 11 (2013) 058; P. Bandyopadhyay,

Higgs production in *CP*-violating supersymmetric cascade decays: Probing the "open hole" at the Large Hadron Collider, J. High Energy Phys. 08 (2011) 016; P. Bandyopadhyay, A. Datta, A. Datta, and B. Mukhopadhyaya, Associated Higgs production in *CP*-violating supersymmetry: Probing the "open hole" at the Large Hadron Collider, Phys. Rev. D **78**, 015017 (2008); D. K. Ghosh and S. Moretti, Probing the light neutral Higgs boson scenario of the *CP*-violating MSSM Higgs sector at the LHC, Eur. Phys. J. C **42**, 341 (2005); D. K. Ghosh, R. M. Godbole, and D. P. Roy, Probing the *CP*-violating light neutral Higgs in the charged Higgs decay at the LHC, Phys. Lett. B **628**, 131 (2005); A. Pilaftsis and C. E. M. Wagner, Higgs bosons in the minimal supersymmetric standard model with explicit *CP* violation, Nucl. Phys. **B553**, 3 (1999).